




RESEARCH PAPER



# Discovery of facile amides-functionalized rhodanine-3-acetic acid derivatives as potential anticancer agents by disrupting microtubule dynamics

Xiang Zhou<sup>a,b,\*</sup> , Jiamin Liu<sup>b,\*</sup> , Jiao Meng<sup>a</sup>, Yihong Fu<sup>b</sup>, Zhibin Wu<sup>a</sup>, Guiping Ouyang<sup>b</sup> and Zhenchao Wang<sup>a,b</sup> 

<sup>a</sup>State Key Laboratory Breeding Base of Green Pesticide and Agricultural Bioengineering, Key Laboratory of Green Pesticide and Agricultural Bioengineering, Ministry of Education, Guiyang, People's Republic of China; <sup>b</sup>College of Pharmacy, Guizhou University, Guiyang, People's Republic of China

## ABSTRACT

Microtubule dynamics are crucial for multiple cell functions, and cancer cells are particularly sensitive to microtubule-modulating agents. Here, we describe the design and synthesis of a series of (Z)-2-(5-benzylidene-4-oxo-2-thioxothiazolidin-3-yl)-N-phenylacetamide derivatives and evaluation of their microtubule-modulating and anticancer activities *in vitro*. Proliferation assays identified **I<sub>20</sub>** as the most potent of the antiproliferative compounds, with 50% inhibitory concentrations ranging from 7.0 to 20.3 μM with A549, PC-3, and HepG2 human cancer cell lines. Compound **I<sub>20</sub>** also disrupted cancer A549 cell migration in a concentration-dependent manner. Immunofluorescence microscopy, transmission electron microscopy, and tubulin polymerisation assays suggested that compound **I<sub>20</sub>** promoted protofilament assembly. In support of this possibility, computational docking studies revealed a strong interaction between compound **I<sub>20</sub>** and tubulin Arg β369, which is also the binding site for the anticancer drug Taxol. Our results suggest that (Z)-2-(5-benzylidene-4-oxo-2-thioxothiazolidin-3-yl)-N-phenylacetamide derivatives could have utility for the development of microtubule-stabilising therapeutic agents.

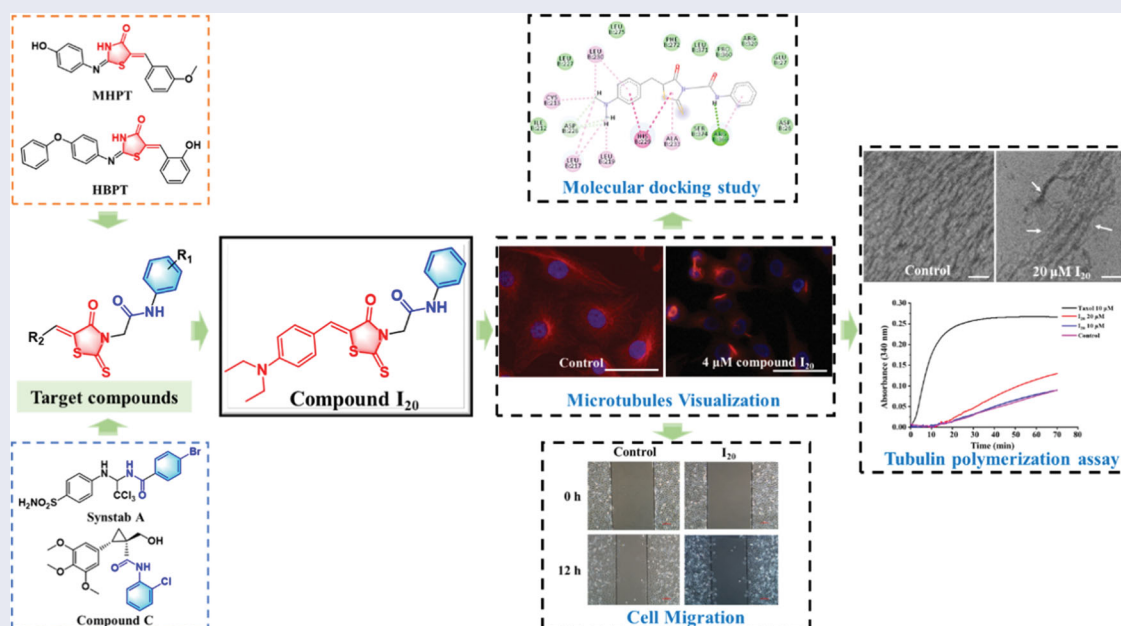
## ARTICLE HISTORY

Received 25 June 2021  
Revised 25 August 2021  
Accepted 27 August 2021

## KEYWORDS

Microtubule; antiproliferative activity; tubulin stabiliser; taxol binding domains

## GRAPHICAL ABSTRACT



## 1. Introduction

Cancer, defined as uncontrolled cell growth, is one of the most common non-infectious diseases and a leading cause of death worldwide<sup>1,2</sup>. In 2020, cancer was estimated to be responsible for

about 10 million deaths globally, and this is expected to increase to approximately 13 million deaths by 2030<sup>3,4</sup>. Although treatment modalities for cancer, including traditional chemotherapy, have advanced considerably in the past decade, the use of many

**CONTACT** Zhenchao Wang  [wzc.4884@163.com](mailto:wzc.4884@163.com)  Guizhou University, Guiyang, People's Republic of China

\*These authors contributed equally to this work.

© 2021 The Author(s). Published by Informa UK Limited, trading as Taylor & Francis Group.

This is an Open Access article distributed under the terms of the Creative Commons Attribution-NonCommercial License (<http://creativecommons.org/licenses/by-nc/4.0/>), which permits unrestricted non-commercial use, distribution, and reproduction in any medium, provided the original work is properly cited.

anticancer drugs is hampered by severe and often debilitating side effects<sup>5-8</sup>. Consequently, the discovery and development of novel small molecule anticancer agents with minimal side effects and low production costs are still challenging.

Disruption of microtubule dynamics has been considered to be an outstanding target for anticancer drug development for decades, due in large part to the crucial functions of microtubules in many fundamental cell processes, including maintenance of cell shape, and cell division, migration, and proliferation<sup>9-12</sup>. Many microtubule-interacting anticancer agents have been developed<sup>12-14</sup> that can be broadly divided into microtubule-stabilising and -destabilising agents according to their effects on microtubule assembly dynamics. These modulators have been shown to bind to tubulin through four main sites, which are referred to as Taxol, laulimalide, vinca alkaloid, and colchicine binding sites<sup>12,15-17</sup>.

Many agents that disrupt cell functions by promoting or inhibiting microtubule assembly dynamics are mainstays of cancer treatment, however, many of them, especially those derived from natural sources, have limited use due to high toxicity, complex isolation processes, and difficulty in obtaining source material<sup>18,19</sup>. Thus, there is an urgent need to develop novel chemically synthetic small molecules that can modulate microtubule dynamics for the treatment of cancer.

The rhodanine scaffold is an important active pharmacophore that can inhibit cell proliferation by interacting with tubulin. Importantly, rhodanine has demonstrated low toxicity against normal cells such as HBPT and MHPT<sup>20,21</sup>. In addition, some compounds bearing  $\alpha$ ,  $\beta$ -unsaturated ketones and derivatives of acrylamide, such as 4'-methoxy-2-styrylchromone and phenylcinnamides, compound A (see Figure 1), and compound B (see Figure 1) often have microtubule-modulating activity<sup>22-25</sup>. Synstab A and the cyclopropylamide analogue compound C (see Figure 1) have also been shown to stabilise microtubule polymerisation<sup>26-28</sup>. These findings suggest that compounds based on a rhodanine scaffold,  $\alpha$ ,  $\beta$ -unsaturated ketones, and acrylamide derivatives, all of which have relatively simple synthetic routes, exhibit anticancer

activity by targeting tubulin. Therefore, we combined the core pharmacophores of a rhodanine scaffold,  $\alpha$ ,  $\beta$ -unsaturated ketones, and acrylamide derivatives as a possible strategy to develop novel microtubule-interacting agents.

In this article, a series of facile amides-functionalized rhodanine-3-acetic acid derivatives (Figure 1) were designed, synthesised, and exploited the antiproliferative activity *in vitro*. Moreover, the mechanism of targeting tubulin will be further investigated.

## 2. Results and discussion

### 2.1. Compound synthesis

A simple synthetic route was designed for preparing the target compounds (Scheme 1). The structures of title compounds were confirmed by NMR and HRMS analysis (Supporting Information).

### 2.2. Antiproliferative activity of compounds I<sub>1</sub>-I<sub>34</sub> *in vitro*

Rhodanine-3-acetic acid derivatives I<sub>1</sub>-I<sub>34</sub> were examined for their effect on the proliferation of three human cancer cell lines: A549 (lung adenocarcinoma), PC-3 (prostate cancer), and HepG2 (hepatocellular carcinoma), using the 3-(4,5-dimethylthiazol-2-yl)-2, 5-diphenyltetrazolium bromide (MTT) cell proliferation assay. The microtubule polymerisation inhibitor colchicine and the tyrosine kinase inhibitor gefitinib served as reference compounds. The inhibitory activity of the compounds was first assessed at a fixed concentration of 10  $\mu$ M (Table 1). Compounds I<sub>1</sub>, I<sub>19</sub>, and I<sub>20</sub> exhibited the best antiproliferative activities against A549 and PC-3 cancer cells, and the activities were similar to that achieved with gefitinib. Compounds I<sub>1</sub>, I<sub>4</sub>, I<sub>5</sub>, I<sub>6</sub>, I<sub>11</sub>, I<sub>16</sub>, and I<sub>19</sub> demonstrated good antiproliferative activity against HepG2 cancer cells, and their activities were slightly better than gefitinib. These results suggested that the compound series had superior antiproliferative activity against A549 and PC-3 than HepG2 cancer cells (Table 1).

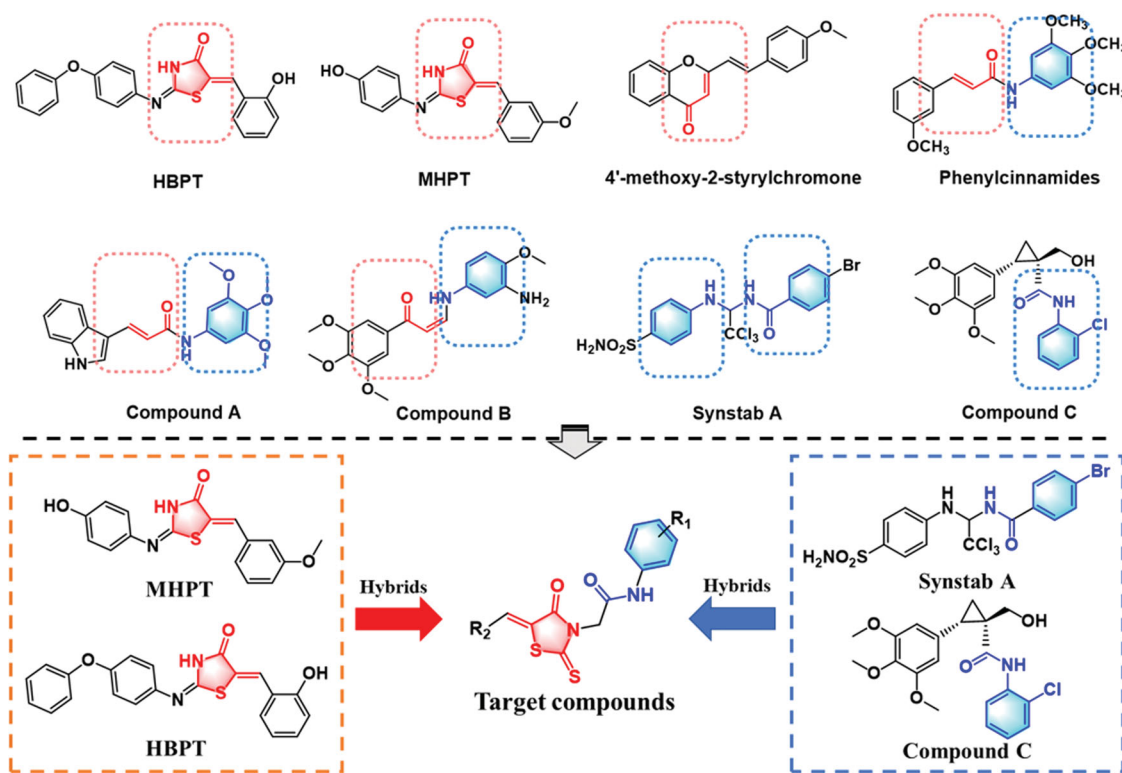


Figure 1. Molecular structures of current microtubule-interacting agents and the related design concept of target molecules.

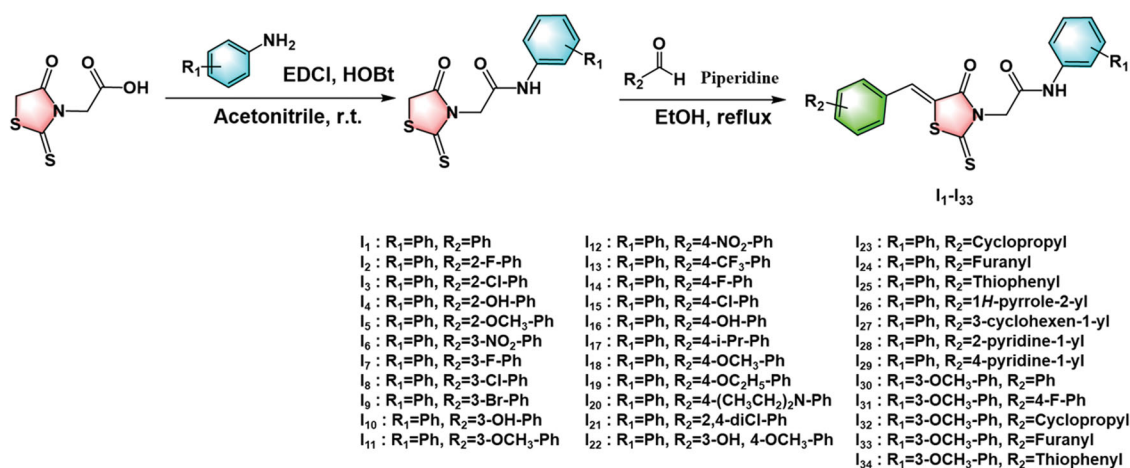
Scheme 1. Synthetic route for the target molecules  $I_1$ - $I_{34}$ .

Table 1. The antiproliferative activities of all designed compounds against cancer cell lines

No.	$R_1$	$R_2$	10 $\mu$ M (%inhibition $\pm$ SD) <sup>a</sup>		
			A549	PC-3	HepG2
$I_1$	Ph	Ph	43.3 $\pm$ 7.05	43.8 $\pm$ 7.39	31.3 $\pm$ 3.40
$I_2$	Ph	2-F-Ph	13.5 $\pm$ 5.94	16.8 $\pm$ 6.31	7.65 $\pm$ 2.81
$I_3$	Ph	2-Cl-Ph	20.5 $\pm$ 5.22	22.6 $\pm$ 8.86	11.0 $\pm$ 1.09
$I_4$	Ph	2-OH-Ph	34.5 $\pm$ 3.28	36.2 $\pm$ 1.31	26.4 $\pm$ 6.99
$I_5$	Ph	2-OCH <sub>3</sub> -Ph	38.3 $\pm$ 7.94	29.0 $\pm$ 5.76	25.6 $\pm$ 8.29
$I_6$	Ph	3-NO <sub>2</sub> -Ph	22.2 $\pm$ 2.04	17.6 $\pm$ 4.41	24.2 $\pm$ 2.85
$I_7$	Ph	3-F-Ph	26.1 $\pm$ 9.76	18.9 $\pm$ 7.80	7.27 $\pm$ 3.65
$I_8$	Ph	3-Cl-Ph	25.9 $\pm$ 1.12	21.0 $\pm$ 4.22	10.0 $\pm$ 8.58
$I_9$	Ph	3-Br-Ph	25.8 $\pm$ 5.96	27.3 $\pm$ 1.24	12.7 $\pm$ 7.10
$I_{10}$	Ph	3-OH-Ph	14.5 $\pm$ 3.41	12.6 $\pm$ 4.02	5.11 $\pm$ 0.69
$I_{11}$	Ph	3-OCH <sub>3</sub> -Ph	25.7 $\pm$ 3.07	10.6 $\pm$ 2.99	13.9 $\pm$ 9.39
$I_{12}$	Ph	4-NO <sub>2</sub> -Ph	24.4 $\pm$ 1.08	16.6 $\pm$ 3.30	22.6 $\pm$ 0.65
$I_{13}$	Ph	4-CF <sub>3</sub> -Ph	27.8 $\pm$ 2.77	32.1 $\pm$ 4.62	11.2 $\pm$ 7.48
$I_{14}$	Ph	4-F-Ph	27.6 $\pm$ 2.76	27.7 $\pm$ 7.29	6.59 $\pm$ 1.11
$I_{15}$	Ph	4-Cl-Ph	36.7 $\pm$ 4.78	32.3 $\pm$ 4.36	21.2 $\pm$ 6.19
$I_{16}$	Ph	4-OH-Ph	29.6 $\pm$ 3.04	24.9 $\pm$ 4.03	31.6 $\pm$ 4.35
$I_{17}$	Ph	4-i-pr-Ph	22.5 $\pm$ 4.54	29.0 $\pm$ 7.01	17.5 $\pm$ 4.07
$I_{18}$	Ph	4-OCH <sub>3</sub> -Ph	23.0 $\pm$ 5.90	25.0 $\pm$ 4.85	13.6 $\pm$ 2.39
$I_{19}$	Ph	4-OC <sub>2</sub> H <sub>5</sub> -Ph	48.2 $\pm$ 5.78	38.0 $\pm$ 9.31	34.3 $\pm$ 5.88
$I_{20}$	Ph	4-(CH <sub>3</sub> CH <sub>2</sub> ) <sub>2</sub> N-Ph	58.8 $\pm$ 3.68	10.1 $\pm$ 4.06	9.79 $\pm$ 2.24
$I_{21}$	Ph	2,4-diCl-Ph	4.43 $\pm$ 1.21	19.2 $\pm$ 8.28	8.03 $\pm$ 3.03
$I_{22}$	Ph	3-OH-4-OCH <sub>3</sub> -Ph	5.02 $\pm$ 2.21	7.78 $\pm$ 5.71	5.04 $\pm$ 5.36
$I_{23}$	Ph	Cyclopropyl	28.9 $\pm$ 5.40	24.1 $\pm$ 1.08	11.0 $\pm$ 7.62
$I_{24}$	Ph	Furanyl	39.5 $\pm$ 5.75	23.1 $\pm$ 8.45	18.6 $\pm$ 3.86
$I_{25}$	Ph	Thiophenyl	23.5 $\pm$ 3.04	5.30 $\pm$ 2.26	11.8 $\pm$ 2.60
$I_{26}$	Ph	1H-Pyrrole-2-yl	21.4 $\pm$ 5.99	22.7 $\pm$ 7.31	9.65 $\pm$ 2.44
$I_{27}$	Ph	3-Cyclohexen-1-yl	19.6 $\pm$ 3.88	18.9 $\pm$ 6.58	5.31 $\pm$ 1.20
$I_{28}$	Ph	2-Pyridine-1-yl	32.6 $\pm$ 4.59	30.5 $\pm$ 2.47	10.2 $\pm$ 3.30
$I_{29}$	Ph	4-Pyridine-1-yl	25.9 $\pm$ 5.70	5.33 $\pm$ 2.26	11.8 $\pm$ 2.60
$I_{30}$	3-OCH <sub>3</sub> -Ph	Ph	26.3 $\pm$ 1.68	17.83 $\pm$ 7.74	11.8 $\pm$ 0.64
$I_{31}$	3-OCH <sub>3</sub> -Ph	4-F-Ph	22.3 $\pm$ 1.82	13.02 $\pm$ 7.60	10.2 $\pm$ 4.22
$I_{32}$	3-OCH <sub>3</sub> -Ph	Cyclopropyl	17.2 $\pm$ 2.69	18.6 $\pm$ 2.52	12.1 $\pm$ 3.21
$I_{33}$	3-OCH <sub>3</sub> -Ph	Furanyl	13.7 $\pm$ 3.30	8.63 $\pm$ 2.43	5.43 $\pm$ 1.12
$I_{34}$	3-OCH <sub>3</sub> -Ph	Thiophenyl	12.4 $\pm$ 4.84	7.28 $\pm$ 6.09	12.2 $\pm$ 4.01
Colchicine			68.5 $\pm$ 6.61	58.6 $\pm$ 4.51	56.4 $\pm$ 1.51
Gefitinib			56.5 $\pm$ 4.73	54.5 $\pm$ 3.59	29.1 $\pm$ 4.98

<sup>a</sup>The antiproliferative activities of all target compounds against cancer cell lines were determined by MTT assay. The data represent the mean of triplicate determinations.

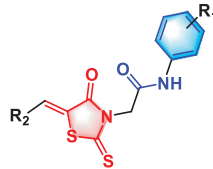
To further analyse the structure–activity relationships (SARs) of the compounds, dose-response proliferation assays were performed to enable calculation of the concentration of each compound yielding 50% maximal inhibition ( $IC_{50}$ ) of cell proliferation. Table 2 shows the  $IC_{50}$  values of all title compounds. Compound  $I_{20}$  ( $R_1=Ph$ ,  $R_2=4-(CH_3CH_2)_2N-Ph$ ) remained the most potent antiproliferative compound against A549 cancer lines and had an  $IC_{50}$  of 7.0  $\mu$ M, which was approximately equal to the potency of gefitinib ( $IC_{50} = 5.89 \mu$ M). Compounds  $I_4$ ,  $I_5$ ,  $I_{15}$ ,  $I_{16}$ ,  $I_{19}$ ,  $I_{23}$ ,  $I_{24}$ ,  $I_{25}$ ,  $I_{28}$ ,  $I_{31}$ , and  $I_{34}$  had moderate antiproliferative activity for A 459 cells with  $IC_{50}$  values ranging between 10.3  $\mu$ M ( $I_{19}$ ) and 17.8  $\mu$ M ( $I_{34}$ ), which was about an order of magnitude less potent than colchicine ( $IC_{50} = 1.42 \mu$ M). The SAR of the compounds for inhibition of A549 proliferation can be summarised as follows: (1) a bulky electron-withdrawing group at the ortho-position was unfavourable, as shown by compound  $I_2$  (2-OCH<sub>3</sub>-Ph, 13.4  $\mu$ M),  $I_3$  (2-OH-Ph, 15.8  $\mu$ M),  $I_2$  (2-F-Ph, 22.7  $\mu$ M), and  $I_3$  (2-Cl-Ph, 42.1  $\mu$ M); (2) a bulky electron-withdrawing group at the meta-position was beneficial, as shown by compound  $I_7$  (3-F-Ph, 29.6  $\mu$ M) and  $I_9$  (3-Br-Ph, 25.5  $\mu$ M); (3) a bulky steric-hindering group at the para position was associated with good bioactivity, as shown by compound  $I_{15}$  (4-Cl-Ph, 14.3  $\mu$ M),  $I_{19}$  (4-OC<sub>2</sub>H<sub>5</sub>-Ph, 10.3  $\mu$ M),  $I_{20}$  (4-(CH<sub>3</sub>CH<sub>2</sub>)<sub>2</sub>N-Ph, 7.00  $\mu$ M),  $I_{14}$  (4-F-Ph, 18.8  $\mu$ M),  $I_{16}$  (4-OH-Ph, 16.8  $\mu$ M), and  $I_{18}$  (4-OCH<sub>3</sub>-Ph, 25.7  $\mu$ M); and (4) introduction of a methoxyl group at the meta-position on the benzyl group of  $R_1$  was detrimental, as shown by compound  $I_1$  ( $R_1=Ph$ ,  $R_2=Ph$ , 11.3  $\mu$ M),  $I_{30}$  ( $R_1=3-OCH_3-Ph$ ,  $R_2=Ph$ , 22.1  $\mu$ M),  $I_{23}$  ( $R_1=Ph$ ,  $R_2=cyclopropyl$ , 15.7  $\mu$ M),  $I_{32}$  ( $R_1=3-OCH_3-Ph$ ,  $R_2=cyclopropyl$ , 39.1  $\mu$ M),  $I_{24}$  ( $R_1=Ph$ ,  $R_2=furanyl$ , 14.9  $\mu$ M), and  $I_{34}$  ( $R_1=3-OCH_3-Ph$ ,  $R_2=furanyl$ , 46.5  $\mu$ M).

We next examined the selectivity of the compounds towards cancer cell lines by examining the proliferation of the normal rat kidney cell line NRK-52E. Many of the compounds were cytotoxic to NRK-52E cells (Table 3), indicating poor selectivity. However, compound  $I_{20}$ , which exhibited strong antiproliferative activity with A549 cells ( $IC_{50}=7.00 \mu$ M), was only weakly cytotoxic towards NRK-52E cells ( $IC_{50}=14.7 \mu$ M and SI = 2.10). Therefore, we selected compound  $I_{20}$  for further investigation. selectivity

### 2.3. Immunofluorescence staining of tubulin and the effect of $I_{20}$ on microtubule dynamics

To determine the mechanism underlying the antiproliferative activity of compound  $I_{20}$ , A549 cells were treated with 0 (DMSO),

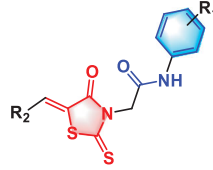
**Table 2.** The antiproliferative activities of all designed compounds against A549 cells.



No.	R <sub>1</sub>	R <sub>2</sub>	IC <sub>50</sub> (μM) A549
I <sub>1</sub>	Ph	Ph	11.3 ± 1.50
I <sub>2</sub>	Ph	2-F-Ph	22.7 ± 5.45
I <sub>3</sub>	Ph	2-Cl-Ph	42.1 ± 4.73
I <sub>4</sub>	Ph	2-OH-Ph	15.8 ± 3.03
I <sub>5</sub>	Ph	2-OCH <sub>3</sub> -Ph	13.4 ± 1.23
I <sub>6</sub>	Ph	3-NO <sub>2</sub> -Ph	22.9 ± 2.07
I <sub>7</sub>	Ph	3-F-Ph	29.6 ± 3.72
I <sub>8</sub>	Ph	3-Cl-Ph	31.0 ± 2.21
I <sub>9</sub>	Ph	3-Br-Ph	25.5 ± 1.24
I <sub>10</sub>	Ph	3-OH-Ph	42.8 ± 6.50
I <sub>11</sub>	Ph	3-OCH <sub>3</sub> -Ph	32.0 ± 5.00
I <sub>12</sub>	Ph	4-NO <sub>2</sub> -Ph	23.6 ± 3.00
I <sub>13</sub>	Ph	4-CF <sub>3</sub> -Ph	20.1 ± 3.13
I <sub>14</sub>	Ph	4-F-Ph	18.8 ± 3.31
I <sub>15</sub>	Ph	4-Cl-Ph	14.3 ± 3.42
I <sub>16</sub>	Ph	4-OH-Ph	16.8 ± 3.66
I <sub>17</sub>	Ph	4-i-pr-Ph	20.7 ± 3.33
I <sub>18</sub>	Ph	4-OCH <sub>3</sub> -Ph	25.7 ± 3.38
I <sub>19</sub>	Ph	4-OC <sub>2</sub> H <sub>5</sub> -Ph	10.3 ± 1.54
I <sub>20</sub>	Ph	4-(CH <sub>3</sub> CH <sub>2</sub> ) <sub>2</sub> N-Ph	7.00 ± 1.06
I <sub>21</sub>	Ph	2,4-diCl-Ph	36.9 ± 1.36
I <sub>22</sub>	Ph	3-OH-4-OCH <sub>3</sub> -Ph	84.9 ± 9.00
I <sub>23</sub>	Ph	Cyclopropyl	15.7 ± 0.98
I <sub>24</sub>	Ph	Furanyl	14.9 ± 1.72
I <sub>25</sub>	Ph	Thiophenyl	16.0 ± 3.46
I <sub>26</sub>	Ph	1 <i>H</i> -Pyrrole-2-yl	20.0 ± 4.25
I <sub>27</sub>	Ph	3-Cyclohexen-1-yl	51.3 ± 9.09
I <sub>28</sub>	Ph	2-Pyridine-1-yl	17.3 ± 3.90
I <sub>29</sub>	Ph	4-Pyridine-1-yl	26.4 ± 8.00
I <sub>30</sub>	3-OCH <sub>3</sub> -Ph	Ph	22.1 ± 3.41
I <sub>31</sub>	3-OCH <sub>3</sub> -Ph	4-F-Ph	14.4 ± 0.70
I <sub>32</sub>	3-OCH <sub>3</sub> -Ph	Cyclopropyl	39.1 ± 5.62
I <sub>33</sub>	3-OCH <sub>3</sub> -Ph	Furanyl	46.5 ± 7.31
I <sub>34</sub>	3-OCH <sub>3</sub> -Ph	Thiophenyl	17.8 ± 3.75
Colchicine			1.42 ± 0.13
Gefitinib			5.89 ± 1.05

<sup>a</sup>The antiproliferative activities of all target compounds against cancer cell lines were determined by MTT assay. The data represent the mean of triplicate determinations.

**Table 3.** The antiproliferative activities of compounds I<sub>1</sub>, I<sub>5</sub>, I<sub>15</sub>, I<sub>19</sub>, I<sub>20</sub> and I<sub>24</sub> against cancer cell lines and normal cells.



No.	R <sub>1</sub>	R <sub>2</sub>	IC <sub>50</sub> (%inhibition ± SD) <sup>a</sup>				
			A549	PC-3	HepG2	NRK-52E	SI <sup>b</sup>
I <sub>1</sub>	Ph	Ph	11.3 ± 1.50	21.7 ± 2.89	24.7 ± 8.91	13.1 ± 3.58	1.16
I <sub>5</sub>	2-OCH <sub>3</sub> -Ph	Ph	13.4 ± 5.03	14.5 ± 1.30	36.4 ± 8.00	17.4 ± 4.57	1.30
I <sub>15</sub>	4-Cl-Ph	Ph	14.3 ± 3.42	17.6 ± 2.51	20.6 ± 5.19	15.1 ± 2.45	1.06
I <sub>19</sub>	4-OC <sub>2</sub> H <sub>5</sub> -Ph	Ph	10.3 ± 1.54	18.1 ± 3.68	18.8 ± 5.40	11.0 ± 3.10	1.07
I <sub>20</sub>	4-(CH <sub>3</sub> ) <sub>2</sub> N-Ph	Ph	7.00 ± 1.06	19.9 ± 5.56	20.3 ± 2.93	14.7 ± 1.58	2.10
I <sub>24</sub>	Furanyl	Ph	14.9 ± 1.72	25.1 ± 3.39	17.7 ± 2.27	20.1 ± 2.12	1.35
Colchicine			1.42 ± 0.13	1.93 ± 0.28	3.87 ± 0.22	3.21 ± 0.67	2.26
Gefitinib			5.89 ± 1.05	6.99 ± 1.52	19.08 ± 4.98	23.4 ± 4.46	3.97

<sup>a</sup>The antiproliferative activities of all target compounds against cancer cell lines were determined by MTT assay. The data represent the mean of triplicate determinations.

<sup>b</sup>SI: selectivity index. It was calculated as: SI = IC<sub>50</sub>(NRK-52E)/IC<sub>50</sub>(A549).

4, and 8 μM compound I<sub>20</sub> for 48 h, and the cells were then fixed and immunostained for α-tubulin (red fluorescence, Figure 2) and counterstained with DAPI to visualise nuclei (blue fluorescence, Figure 2). Fluorescence patterns showed that DMSO-treated cells displayed uncondensed chromosomes, were in interphase of the cell division cycle, and had microtubules uniformly dispersed in the cytoplasm. In contrast, cells treated with compound I<sub>20</sub> displayed more disordered dispersal of microtubules in the cytoplasm and more condensed chromosomes. Moreover, the microtubule density was reduced and the networks more disorganised in compound I<sub>20</sub>-incubated cells compared with the control cells. These observations indicated that compound I<sub>20</sub> disrupted the microtubule dynamics and morphology of A549 cells, suggesting that this compound may target tubulin.

#### 2.4. Effect of I<sub>20</sub> on tubulin polymerisation in vitro

To determine whether compound I<sub>20</sub> affects microtubule organisation *via* tubulin, we next performed a tubulin polymerisation assay<sup>29–32</sup> using Taxol as the reference microtubule-stabilising agent. As shown in Figure 3, compound I<sub>20</sub> promoted tubulin stabilisation in a concentration-dependent manner. These findings were consistent with the fluorescence microscopy observations and further suggest that compound I<sub>20</sub> stimulates tubulin polymerisation.

#### 2.5. Visualisation of tubulin assembly

Transmission electron microscopy (TEM) was carried out to directly visualise the impact of compound I<sub>20</sub> on tubulin assembly. Using the same conditions as the tubulin polymerisation assay described above, untreated control tubulin demonstrated spontaneous formation of uniform protofilaments, as expected (Figure 4(A)). However, preincubation of the tubulin with 20 μM I<sub>20</sub> induced tubulin polymerisation and created large, nonlinear, disorganised aggregates (Figure 4(B)). TEM imaging thus revealed that compound I<sub>20</sub> could stabilise protofilaments, further supporting the results of the fluorescence microscopy and tubulin assembly assays.

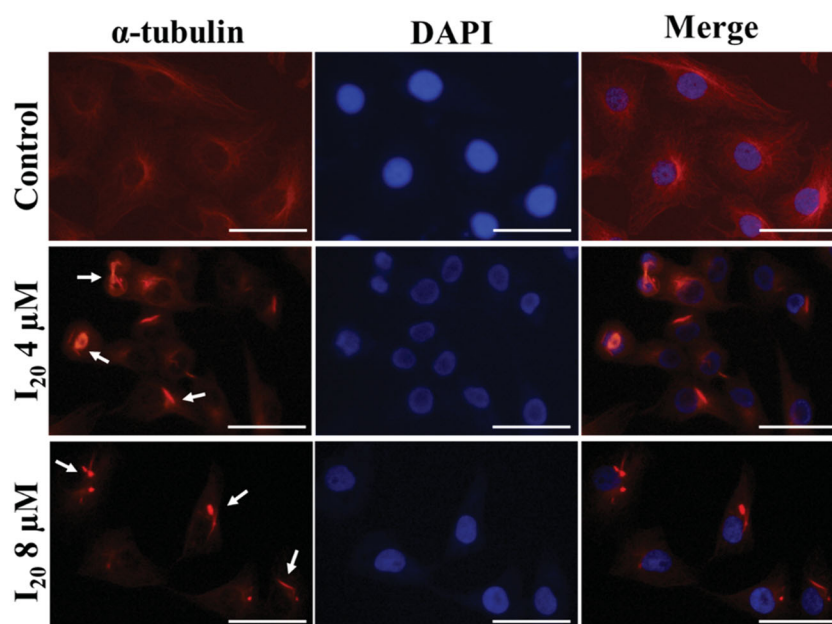


**Figure 2.** Effects of compound  $I_{20}$  on the cellular microtubule network were visualised by immunofluorescence assay. A549 cells were treated with vehicle control 0.1% DMSO, 4  $\mu$ M and 8  $\mu$ M compound  $I_{20}$  for 48 h. Then, cells were fixed and stained with anti- $\alpha$ -tubulin antibody (red fluorescence) and counterstained with DAPI (blue fluorescence). Detection of the fixed and stained cells was performed using fluorescence microscope. Scale bars are 50  $\mu$ m.

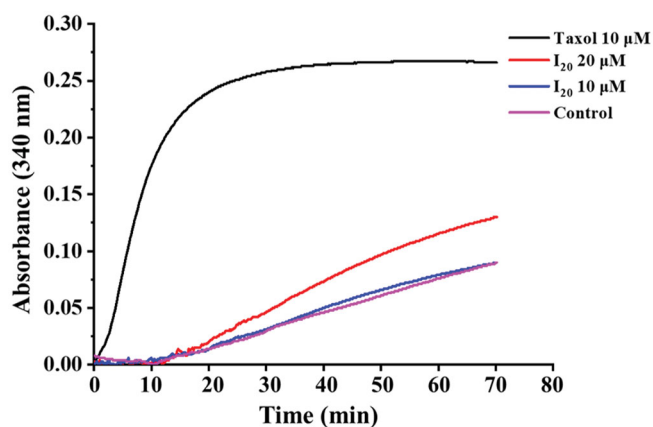


**Figure 3.** Progress of tubulin polymerisation in the presence of 10  $\mu$ M and 20  $\mu$ M compound  $I_{20}$ . Taxol (10  $\mu$ M) was used as positive polymerisation control, whereas untreated tubulin was used as negative control.

## 2.6. Cell cycle analysis

Microtubules form the structural basis of the mitotic spindle, which is a pivotal structure in the process of cell division of eukaryotic cells<sup>33–36</sup>. Therefore, we next examined the effects of compound  $I_{20}$  on the A549 cell cycle. For these experiments, A549 cells were treated with compound  $I_{20}$  at 0, 4  $\mu$ M, and 8  $\mu$ M for 24 h and then incubated with propidium iodide, a red fluorescent dye that binds stoichiometrically to DNA, thereby enabling quantification of DNA at different stages of the cell cycle using flow cytometry. Consistent with the activity of a microtubule-stabilising agent, compound  $I_{20}$  incubation caused an arrest of A549 cells at G2/M. The percentage of cells in G2/M was increased from a baseline of 5.94% of cells after incubation with DMSO to 10.92% and 15.45% for cells incubated with compound  $I_{20}$  at 4 and 8  $\mu$ M, respectively (Figure 5). Taken together, these results validate the antimitotic activity of compound  $I_{20}$  and are consistent with cell cycle arrest induced by disordered microtubule assembly.

## 2.7. Computational docking studies

To better elucidate the binding mode of compound  $I_{20}$  in the active site of tubulin, we performed a molecular docking study with SYBYL-X 2.0 software. Briefly, the reported crystal structure of tubulin (PDB code: 5syf) was employed as the receptor and ligand Taxol was removed from tubulin. Subsequently, the highest docking score conformation of compound  $I_{20}$  in the active site of tubulin derived from the Surflex-Dock Geom module was selected as the preferred binding mode. As depicted in Figure 6, compound  $I_{20}$  occupied the same active pocket as the reference drug Taxol, and the interaction with tubulin involved amino acid residues Asp  $\beta$ 26, Glu  $\beta$ 27, Ile  $\beta$ 212, Cys  $\beta$ 213, Leu  $\beta$ 217, Leu  $\beta$ 219, Asp  $\beta$ 226, Leu  $\beta$ 227, His  $\beta$ 229, Leu  $\beta$ 230, Ala  $\beta$ 233, Phe  $\beta$ 272, Leu  $\beta$ 275, Arg  $\beta$ 320, Pro  $\beta$ 360, Arg  $\beta$ 369, Leu  $\beta$ 371, and Ser  $\beta$ 374. Additionally, although conventional hydrogen bonds were crucial to the interaction, non-covalent interactions (such as  $\pi$ - $\pi$  stacked,  $\pi$ -alkyl, and others) also contributed to the interaction<sup>37–41</sup>. For instance, one hydrogen bond was formed between the -NH group of compound  $I_{20}$  and Arg  $\beta$ 369 of tubulin (2.5 Å). Moreover, Asp  $\beta$ 226 residues formed carbon-hydrogen interactions with the N(CH<sub>3</sub>CH<sub>2</sub>)<sub>2</sub> group of compound  $I_{20}$ . Compound  $I_{20}$  interacted with tubulin residues Asp  $\beta$ 26, Glu  $\beta$ 27, Ile  $\beta$ 212, Asp  $\beta$ 226, Leu  $\beta$ 227, Phe  $\beta$ 272, Leu  $\beta$ 275, Arg  $\beta$ 320, Pro  $\beta$ 360, Leu  $\beta$ 371, and Ser  $\beta$ 374 mainly through van der Waals interactions. A  $\pi$ - $\pi$  stacked interaction was displayed between compound  $I_{20}$  and tubulin His  $\beta$ 229. Finally, amino acid residues Cys  $\beta$ 213, Leu  $\beta$ 217, Leu  $\beta$ 219, Leu  $\beta$ 230, and Ala  $\beta$ 233 interacted with compound  $I_{20}$  through  $\pi$ -alkyl or alkyl interactions. These results suggested that compound  $I_{20}$  promoted microtubule assembly by binding strongly to the Taxol-binding site of tubulin.

## 2.8. Effects on cell migration of compound $I_{20}$

Finally, we examined the ability of compound  $I_{20}$  to influence A549 cell migration, which is an important malignant behaviour and contributes to metastasis, a major cause of cancer-related death<sup>42</sup>. Furthermore, many tubulin-binding agents have been

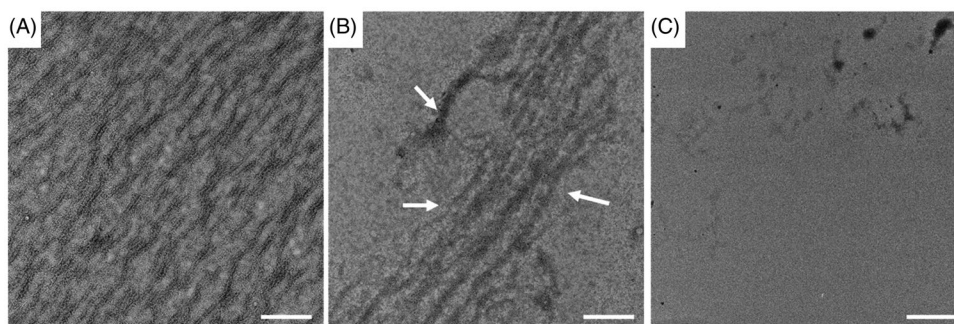


**Figure 4.** Effect of different concentrations of compound  $I_{20}$  on tubulin polymerisation: a) 4 mg/mL tubulin, b) 20  $\mu$ M compound  $I_{20}$  + 4 mg/mL tubulin, c) 20  $\mu$ M compound  $I_{20}$  without tubulin. Scale bars are 1  $\mu$ m.

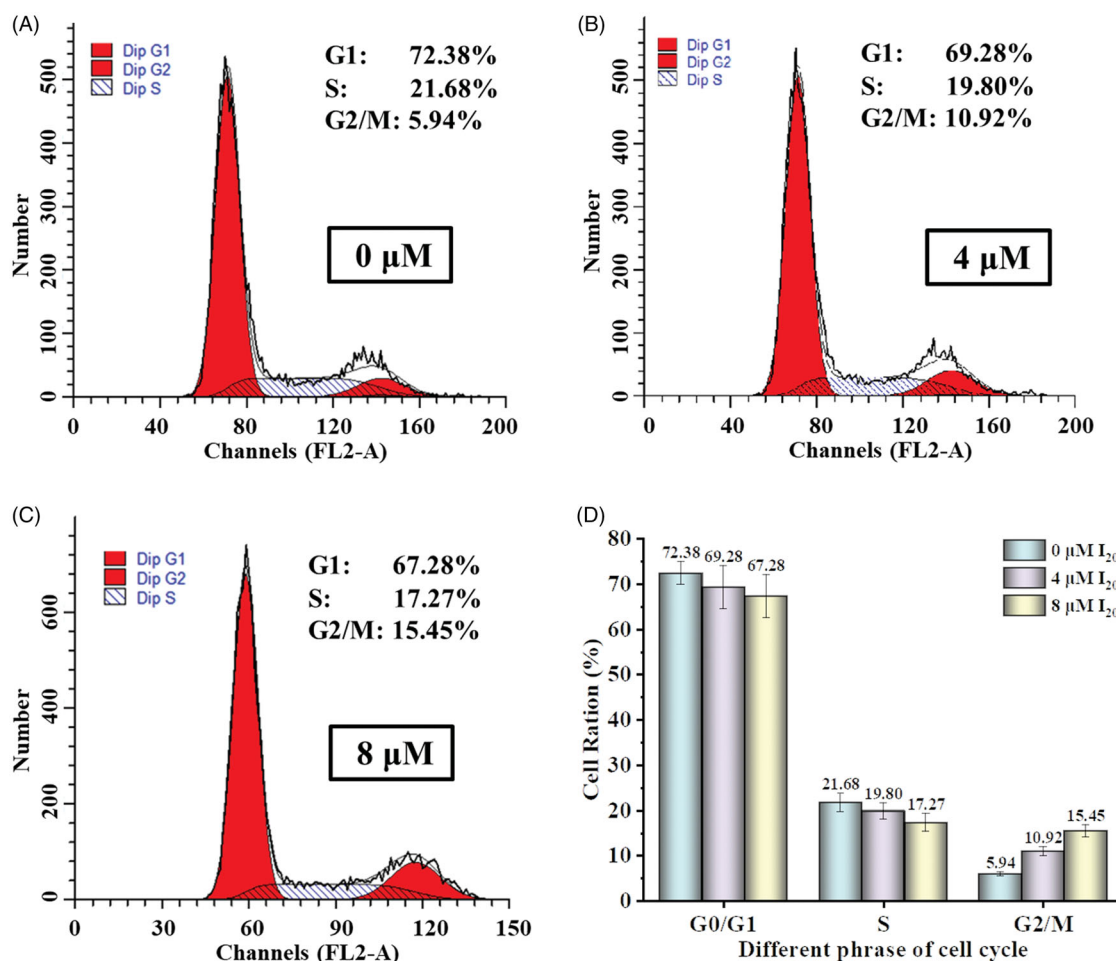


**Figure 5.** The effects of cell cycle affected by compound  $I_{20}$  in A549 cells. (A) DMSO-treated (0.1%) cells served as a control. (B) A549 cells were harvested after incubating with 4  $\mu$ M compound  $I_{20}$ . (C) A549 cells were harvested after incubating with 8  $\mu$ M compound  $I_{20}$ . (D) Cell cycle contributions resulting from treatment with 0  $\mu$ M compound  $I_{20}$  (control) and cells treated with compound  $I_{20}$  (4 and 8  $\mu$ M) for 24 h.

shown to inhibit cancer cell migration<sup>43–45</sup>. The effect of compound  $I_{20}$  on A549 cell migration was measured using wound-healing migration assays. As shown in Figure 7, after 12 h incubation, DMSO-treated control cells exhibited a 26.9% migration rate compared with 17.3% for cells treated with 10  $\mu$ M compound  $I_{20}$ . Similarly, after 48 h incubation, the migration rates were 46.2% for control cells and 26.1% for cells treated with compound  $I_{20}$ . These results demonstrate that the microtubule-stabilising compound  $I_{20}$  can effectively inhibit the migration and proliferation of cancer cells.

### 3. Conclusions

The present study describes the facile preparation of (Z)-2-(5-benzylidene-4-oxo-2-thioxothiazolidin-3-yl)-N-phenylacetamide derivatives with antiproliferative activity against various cancer cells. Notably, compound  $I_{20}$  had excellent antiproliferative activity against A549 cells but was only weakly cytotoxic towards normal NRK-52E cells. Compound  $I_{20}$  was shown to promote microtubule protofilament assembly, leading to reduced microtubule density and disordered networks, and this was confirmed by direct

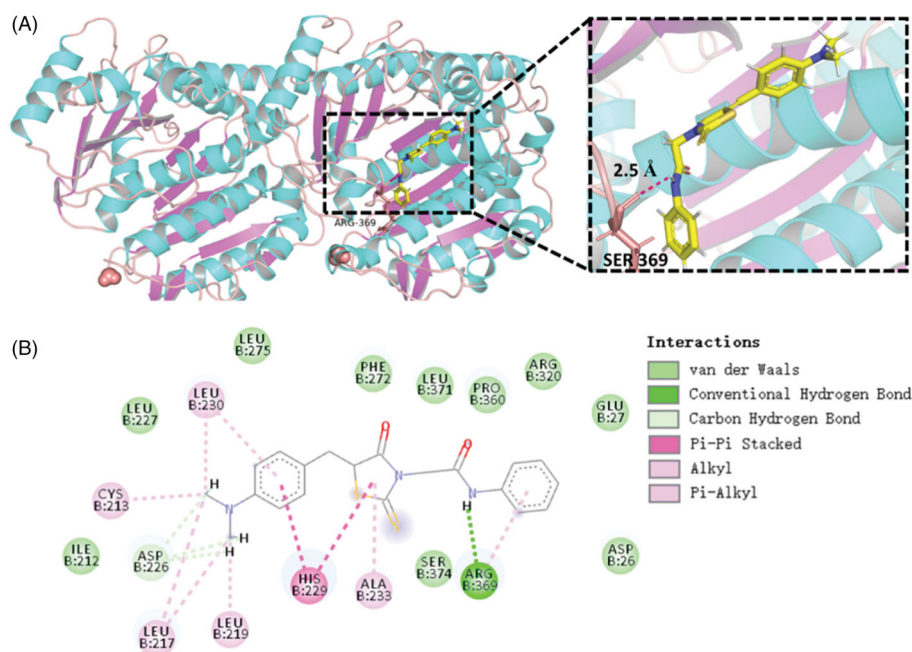


**Figure 6.** Putative binding model of compound **I**<sub>20</sub> with tubulin. (A) Binding of compound **I**<sub>20</sub> into the active site of tubulin was displayed by PyMol software; (B) 2D model of interaction between tubulin and compound **I**<sub>20</sub> using Discovery Studio 4.5 software.

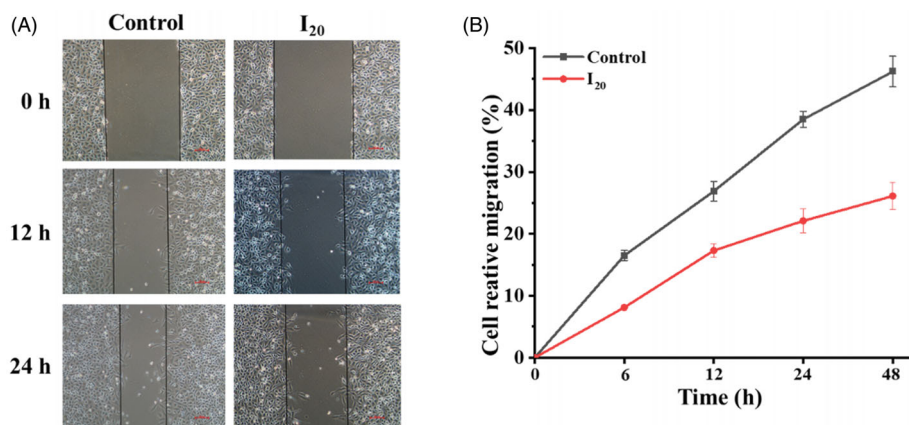


**Figure 7.** Cell migration assay showed that compound **I**<sub>20</sub> inhibited the migration of A549 cells. (A) Cell migration was detected using a wound healing assay in untreated cells (left panel) and cells treated with 10  $\mu$ M compound **I**<sub>20</sub> (right panel) during 24 h. Scale bars are 100  $\mu$ m. (B) The cell relative migration was quantified using the software.

assessment of tubulin polymerisation and by visualisation with TEM. Moreover, compound **I**<sub>20</sub> induced cell cycle arrest of A549 cells and significantly decreased cell migration in a concentration-dependent manner. Finally, molecular modelling studies predicted that compound **I**<sub>20</sub> interacts strongly with Arg  $\beta$ 369 at the Taxol-binding site of tubulin. Taken together, the results of this study identify this series of synthetic modified (Z)-2-(5-benzylidene-4-oxo-2-thioxothiazolidin-3-yl)-N-phenylacetamide derivatives as potential microtubule-stabilising agents for the treatment of cancer. Studies are ongoing to enhance the selective toxicity of compound **I**<sub>20</sub> for cancer cells compared with normal cells and to improve the tubulin-binding capacity of the compound.

## 4 Experimental

### 4.1. Instruments and chemicals

NMR spectra were performed by JEOL-ECX500 instrument (Akishima, Japan) or Bruker Biospin AG-400 instrument (Bruker

Optics, Germany) using DMSO-*d*<sub>6</sub> as solvent and tetramethylsilane as the internal standard. Melting points were determined on a SGW X-4B microscopic melting point apparatus (Shengguang Instrument Co., Ltd., China) and were uncorrected. HRMS spectra were obtained on Thermo Scientific UltiMate 3000 spectrometer (Waltham, USA) or Waters Xevo G2-S QTOF MS (Waters MS Technologies, Manchester, UK). Immunofluorescence staining assay was performed by tubulin-tracker red kit (Beyotime Institute of Biotechnology, Shanghai, China) and observed using a Nikon ECLIPSE Ti-S fluorescent microscope (Nikon, Japan). The tubulin polymerisation assay was carried out using the tubulin polymerisation assay kit (cytoskeleton, #BK004P) and recorded by Cytation<sup>TM</sup> 5 multi-mode readers (BioTek Instruments, Inc. USA). The rhodamine-3-acetic acid and various amine analogues were purchased from Aladdin Industrial Inc. (Shanghai, China) or Bide Pharmatech Co., Ltd. (Shanghai, China). The FACSCalibur<sup>TM</sup> flow cytometer (Becton Dickinson Immunocytometry Systems, San Jose, CA) was employed to analyse the cell cycle arrest.

## 4.2. Pharmacology

### 4.2.1. Cell culture

PC-3 (Human prostate cancer cell line) cell line was kindly donated by the Key Laboratory of Natural Product Chemistry of the Chinese Academy of Sciences of Guizhou Province; A549 (Human non-small cell lung cancer cell line) cell line was purchased from the Shanghai Cell Bank of the Chinese Academy of Sciences; HepG2 (human liver cancer cell line) and NRK 52E (Normal rat kidney cell line) cell line was kindly provided by Guizhou Medical University. The stock cells were maintained RPMI 1640 or DMEM complete medium.

### 4.2.2. Antiproliferative assay

The antiproliferative activities of target compounds against A549, PC-3, HepG2, and NRK-52E were evaluated using the MTT assay according to the previous articles<sup>46,47</sup>. Briefly, the assay was measured at 490 nm by an Infinite<sup>®</sup> M200 PRO multimode Plate Readers (Tecan Group Ltd., Switzerland). gefitinib, and colchicine were used as positive controls.

### 4.2.3. Immunofluorescence pattern of microtubules dynamics affected by compound I<sub>20</sub>

According to the previous protocol<sup>48,49</sup>, A549 cells were seeded in 6-well plate and incubated overnight. The cells were incubated with DMSO or various concentrations of target compounds. Then, 6-well plates were kept at 37 °C and 5% CO<sub>2</sub> for 48 h. Afterwards, the cells were washed with phosphate-buffered saline (PBS, 10 mM, pH 7.3) and fixed with 4% formaldehyde solution for 15 min, and subsequently washed with 0.1% Triton X-100 in PBS. Subsequently, cells were incubated with diluting tubulin-tracker red for 40 min in a dark environment and washed three times using 0.1% Triton X-100 of PBS, and then stained with DAPI (2 µg/mL). Finally, the results were imaging using a Nikon ECLIPSE Ti-S fluorescent microscope (Nikon Co, Japan).

### 4.2.4. Tubulin polymerisation assay in vitro

The *in vitro* tubulin polymerisation assay was measured according to the protocol of HTS-Tubulin Polymerisation Assay Kit (#BK004P, Cytoskeleton, Inc., Denver, CO) in previous articles<sup>30,31</sup>. Primarily, the 96-well plate was pre-warmed at 37 °C, compounds were dissolved in DMSO to obtain a stock solution. 100 µL 4 mg/mL tubulin was reacted with 0.1% DMSO or various of different concentration of compounds in G-PEM buffer at 37 °C. The results were recorded using at 340 nm each 10 s for 70 min using Cytation<sup>™</sup> 5 multi-mode readers.

### 4.2.5. Visualisation of tubulin assembly in vitro

Briefly, according to the protocol of tubulin polymerisation assay<sup>50,51</sup>, the 100 µL centrifuge tubes were pre-warmed at 37 °C. Then, 20 µL 4 mg/mL tubulin was incubated with final concentration of 20 µM compounds in G-PEM buffer, and the reaction was kept at 37 °C for 30 min. Finally, the formed microtubules were transferred to Formvar-carbon-coated copper grids, negatively stained with 1% phosphotungstic acid, and visualised by transmission electron microscope (TEM).

### 4.2.6. Cell cycle analysis

As previously described<sup>52</sup>, the A549 cells treated with various concentration of target compound for 24 h were carefully collected and washed twice in pre-cooled PBS. Then, the cells were resuspended in 2 ml pre-cooled 70% ethanol solution, subsequently kept 4 °C for overnight. Fixed cells were washed with PBS and incubated with 1 mg/mL RNase A for 30 min at 37 °C. Cell nuclei were stained with 20 mg/mL PI staining solution at 4 °C for 30 min in darkness. Finally, the cell cycle distribution was analysed *via* the FACSCalibur<sup>™</sup> flow cytometer (Becton Dickinson Immunocytometry Systems, San Jose, CA).

### 4.2.7. Computational docking studies

Molecular docking studies were carried out SYBYL-X 2.0 software (Tripos, USA) based on its Surflex-Dock Geom module. Briefly, the crystal structure of tubulin protein in complex with Taxol (PDB code: 5syf) was downloaded from RCSB Protein Data Bank ([www.rcsb.org](http://www.rcsb.org)). Then, all the water molecules and Taxol were eliminated from the protein, subsequently the polar hydrogen atoms were added to the crystal structure. Meanwhile, the ligands were prepared, subsequently energy minimised using the Tripos force field and atomic charges were assigned using Gasteiger-Huckel method. Finally, the docking results were performed by PyMol software and Discovery Studio (DS) 2020<sup>41,53,54</sup>.

### 4.2.8. Scratch test

For cell motility determination<sup>55</sup>, A549 cells with a density of 1 × 10<sup>6</sup> cells/mL were seeded in 6-well plates. After the cells adhered to the wall, three uniform thin lines were drawn in each well by a sterile pipette tip. Subsequently, the medium containing 1% foetal bovine serum (FBS) and different subtoxic concentrations of test compounds were added in wells. After incubating with the different time, the cells were monitored and photographed for wound closure using an inverted fluorescence microscope. Finally, the scratch healing rates were calculated: Migration distance (n h) = edge distance (0 h) – edge distance (12 h or 24 h).

### 4.2.9. General procedure for the synthesis of title compounds

Briefly, rhodanine-3-acetic acid and corresponding amines were dissolved in acetonitrile solution<sup>41,56</sup>. Subsequently, EDCI and HOBT were added in the reaction mixture at room temperature to produce the corresponding intermediates. The reaction mixture was poured into water and extracted three times with ethyl acetate. The organic layer was washed twice with 5% aqueous NaOH solution, 5% aqueous HCl solution and water. Finally, the organic layer was dried by anhydrous sodium sulphate, filtered, and evaporated. The corresponding intermediates were reacted with various aldehydes in ethanol solution, and 10 µL piperidine was then added to the mixture at 100 °C to achieve the crude product. The crude product was filtered and further recrystallised to obtain the target compounds I<sub>1</sub>–I<sub>34</sub>.

#### 4.2.9.1. Synthesis of target compounds

(Z)-2-(5-benzylidene-4-oxo-2-thioxothiazolidin-3-yl)-N-phenylacetamide (I<sub>1</sub>). A yellow solid, yield 75.0%, m.p. 249–250 °C; <sup>1</sup>H NMR (400 MHz, DMSO-d<sub>6</sub>) δ 10.44 (s, 1H, CO–NH–phenyl), 7.91 (s, 1H, CH–phenyl), 7.69 (d, J = 6.9 Hz, 2H, phenyl-2-H + phenyl-6-H), 7.57 (q, J = 15.0, 7.3 Hz, 5H, NH-phenyl-2-H + NH-phenyl-6-H + phenyl-3-H + phenyl-4-H + phenyl-5-H), 7.32 (t, J = 7.9 Hz, 2H, NH-phenyl-3-



H + NH-phenyl-5-H), 7.08 (t,  $J = 7.4$  Hz, 1H, NH-phenyl-4-H), 4.90 (s, 2H, CH<sub>2</sub>-CONH); <sup>13</sup>C NMR (101 MHz, DMSO-d<sub>6</sub>) δ 194.1 (s), 167.1 (s), 163.6 (s), 138.9 (s), 134.1 (s), 133.4 (s), 131.6 (s), 131.2 (s), 130.1 (s), 129.4 (s), 124.2 (s), 122.7 (s), 119.6 (s), 47.2 (s); HRMS (ESI) [M + H]<sup>+</sup> calcd for C<sub>18</sub>H<sub>15</sub>O<sub>2</sub>N<sub>2</sub>S<sub>2</sub>: 355.0692, found: 355.0569.

*(Z)-2-(5-(2-fluorobenzylidene)-4-oxo-2-thioxothiazolidin-3-yl)-N-phenylacetamide (I<sub>2</sub>)*. A yellow solid, yield 63.0%, m.p. 244–245 °C; <sup>1</sup>H NMR (400 MHz, DMSO-d<sub>6</sub>) δ 10.44 (s, 1H, CO-NH-phenyl), 7.84 (s, 1H, CH-phenyl), 7.61 (q,  $J = 14.2, 6.5$  Hz, 2H, phenyl-5-H + phenyl-6-H), 7.55 (d,  $J = 7.6$  Hz, 2H, NH-phenyl-2-H + NH-phenyl-6-H), 7.45–7.38 (m, 2H, phenyl-3-H + phenyl-4-H), 7.32 (t,  $J = 8.0$  Hz, 2H, NH-phenyl-3-H + NH-phenyl-5-H), 7.08 (t,  $J = 7.4$  Hz, 1H, NH-phenyl-4-H), 4.90 (s, 2H, CH<sub>2</sub>-CONH); <sup>13</sup>C NMR (101 MHz, DMSO-d<sub>6</sub>) δ 193.8 (s), 166.9 (s), 163.5 (s), 161.1 (d, <sup>1</sup> $J_{C-F} = 253.1$  Hz), 138.9 (s), 134.0 (d, <sup>4</sup> $J_{C-F} = 9.0$  Hz), 130.2 (s), 129.4 (s), 126.2 (d, <sup>6</sup> $J_{C-F} = 3.4$  Hz), 125.3 (s), 125.1 (d, <sup>5</sup> $J_{C-F} = 6.0$  Hz), 124.2 (s), 121.2 (d, <sup>3</sup> $J_{C-F} = 12.0$  Hz), 119.6 (s), 116.9 (d, <sup>2</sup> $J_{C-F} = 21.3$  Hz), 47.3 (s); HRMS (ESI) [M-H]<sup>-</sup> calcd for C<sub>18</sub>H<sub>12</sub>O<sub>2</sub>N<sub>2</sub>FS<sub>2</sub>: 371.0332, found: 371.0319.

*(Z)-2-(5-(2-chlorobenzylidene)-4-oxo-2-thioxothiazolidin-3-yl)-N-phenylacetamide (I<sub>3</sub>)*. A yellow solid, yield 62.0%, m.p. 241–242 °C; <sup>1</sup>H NMR (400 MHz, DMSO-d<sub>6</sub>) δ 10.44 (s, 1H, CO-NH-phenyl), 7.98 (s, 1H, CH-phenyl), 7.71–7.62 (m, 2H, phenyl-5-H + phenyl-6-H), 7.58–7.52 (m, 4H, NH-phenyl-2-H + NH-phenyl-6-H + phenyl-3-H + phenyl-4-H), 7.32 (t,  $J = 7.9$  Hz, 2H, NH-phenyl-3-H + NH-phenyl-5-H), 7.08 (t,  $J = 7.4$  Hz, 1H, NH-phenyl-4-H), 4.90 (s, 2H, CH<sub>2</sub>-CONH); <sup>13</sup>C NMR (101 MHz, DMSO-d<sub>6</sub>) δ 193.9 (s), 166.8 (s), 163.5 (s), 138.9 (s), 135.3 (s), 133.0 (s), 131.3 (s), 131.0 (s), 130.0 (s), 129.4 (s), 128.9 (s), 128.7 (s), 126.3 (s), 124.2 (s), 119.6 (s), 47.3 (s); HRMS (ESI) [M-H]<sup>-</sup> calcd for C<sub>18</sub>H<sub>12</sub>O<sub>2</sub>N<sub>2</sub>ClS<sub>2</sub>: 387.0038, found: 387.0023.

*(Z)-2-(5-(2-hydroxybenzylidene)-4-oxo-2-thioxothiazolidin-3-yl)-N-phenylacetamide (I<sub>4</sub>)*. A yellow solid, yield 25.0%, m.p. 210–211 °C; <sup>1</sup>H NMR (400 MHz, DMSO-d<sub>6</sub>) δ 10.41 (s, 1H, CO-NH-phenyl), 8.15 (s, 1H, CH-phenyl), 7.74 (dd,  $J = 7.8, 1.4$  Hz, 1H, phenyl-6-H), 7.59 (d,  $J = 1.3$  Hz, 1H, phenyl-4-H), 7.51–7.39 (m, 5H, NH-phenyl-2-H + NH-phenyl-6-H + phenyl-3-H + phenyl-5-H + 2-OH-phenyl), 7.34 (td,  $J = 7.7, 1.0$  Hz, 1H, NH-phenyl-4-H), 7.28 (dd,  $J = 5.3, 3.2$  Hz, 2H, NH-phenyl-3-H + NH-phenyl-5-H), 4.29 (d,  $J = 0.7$  Hz, 2H, CH<sub>2</sub>-CONH); <sup>13</sup>C NMR (101 MHz, DMSO-d<sub>6</sub>) δ 183.8 (s), 172.7 (s), 159.0 (s), 152.4 (s), 137.6 (s), 133.9 (s), 132.1 (s), 129.3 (s), 129.2 (s), 129.0 (s), 128.4 (s), 125.4 (s), 123.7 (s), 119.7 (s), 116.6 (s), 49.6 (s); HRMS (ESI) [M-H]<sup>-</sup> calcd for C<sub>18</sub>H<sub>13</sub>O<sub>3</sub>N<sub>2</sub>S<sub>2</sub>: 369.0380, found: 369.0362.

*(Z)-2-(5-(2-methoxybenzylidene)-4-oxo-2-thioxothiazolidin-3-yl)-N-phenylacetamide (I<sub>5</sub>)*. A yellow solid, yield 84.0%, m.p. 266–267 °C; <sup>1</sup>H NMR (400 MHz, DMSO-d<sub>6</sub>) δ 10.43 (s, 1H, CO-NH-phenyl), 7.99 (s, 1H, CH-phenyl), 7.54 (dd,  $J = 13.4, 5.0$  Hz, 3H, NH-phenyl-2-H + NH-phenyl-6-H + phenyl-6-H), 7.51–7.47 (m, 1H, phenyl-4-H), 7.32 (t,  $J = 7.9$  Hz, 2H, NH-phenyl-3-H + NH-phenyl-5-H), 7.18 (d,  $J = 8.2$  Hz, 1H, phenyl-3-H), 7.13 (t,  $J = 7.5$  Hz, 1H, phenyl-5-H), 7.07 (t,  $J = 7.4$  Hz, 1H, NH-phenyl-4-H), 4.89 (s, 2H, CH<sub>2</sub>-CONH), 3.93 (s, 3H, OCH<sub>3</sub>); <sup>13</sup>C NMR (101 MHz, DMSO-d<sub>6</sub>) δ 194.6 (s), 167.2 (s), 163.7 (s), 158.7 (s), 138.9 (s), 133.9 (s), 130.8 (s), 129.5 (s), 129.4 (s), 124.2 (s), 122.6 (s), 121.8 (s), 121.7 (s), 119.6 (s), 112.6 (s), 56.3 (s), 47.2 (s); HRMS (ESI) [M-H]<sup>-</sup> calcd for C<sub>19</sub>H<sub>15</sub>O<sub>3</sub>N<sub>2</sub>S<sub>2</sub>: 383.0536, found: 383.0519.

*(Z)-2-(5-(3-nitrobenzylidene)-4-oxo-2-thioxothiazolidin-3-yl)-N-phenylacetamide (I<sub>6</sub>)*. A yellow solid, yield 60.0%, m.p. 266–267 °C; <sup>1</sup>H

NMR (400 MHz, DMSO-d<sub>6</sub>) δ 10.45 (s, 1H, CO-NH-phenyl), 8.53 (s, 1H, phenyl-2-H), 8.33 (dd,  $J = 8.3, 1.7$  Hz, 1H, phenyl-4-H), 8.07 (d,  $J = 8.6$  Hz, 2H, CH-phenyl + phenyl-6-H), 7.85 (t,  $J = 8.1$  Hz, 1H, phenyl-6-H), 7.55 (d,  $J = 7.7$  Hz, 2H, NH-phenyl-2-H + NH-phenyl-6-H), 7.32 (t,  $J = 7.9$  Hz, 2H, NH-phenyl-3-H + NH-phenyl-5-H), 7.08 (t,  $J = 7.4$  Hz, 1H, NH-phenyl-4-H), 4.91 (s, 2H, CH<sub>2</sub>-CONH); <sup>13</sup>C NMR (101 MHz, DMSO-d<sub>6</sub>) δ 193.5 (s), 166.9 (s), 163.5 (s), 148.8 (s), 138.9 (s), 136.3 (s), 135.0 (s), 131.6 (s), 129.4 (s), 125.7 (s), 125.6 (s), 125.5 (s), 124.2 (s), 119.6 (s), 47.3 (s); HRMS (ESI) [M-H]<sup>-</sup> calcd for C<sub>18</sub>H<sub>12</sub>O<sub>4</sub>N<sub>3</sub>S<sub>2</sub>: 398.0279, found: 398.0264.

*(Z)-2-(5-(3-fluorobenzylidene)-4-oxo-2-thioxothiazolidin-3-yl)-N-phenylacetamide (I<sub>7</sub>)*. A yellow solid, yield 55.0%, m.p. 259–260 °C; <sup>1</sup>H NMR (400 MHz, DMSO-d<sub>6</sub>) δ 10.44 (s, 1H, CO-NH-phenyl), 7.91 (s, 1H, CH-phenyl), 7.68–7.60 (m, 1H, phenyl-5-H), 7.60–7.53 (m, 3H, NH-phenyl-2-H + NH-phenyl-6-H + phenyl-4-H), 7.51 (d,  $J = 7.9$  Hz, 1H, phenyl-5-H), 7.40 (td,  $J = 8.3, 2.0$  Hz, 1H, phenyl-2-H), 7.33 (t,  $J = 7.9$  Hz, 2H, NH-phenyl-3-H + NH-phenyl-5-H), 7.08 (t,  $J = 7.4$  Hz, 1H, NH-phenyl-4-H), 4.90 (s, 2H, CH<sub>2</sub>-CONH); <sup>13</sup>C NMR (101 MHz, DMSO-d<sub>6</sub>) δ 193.8 (s), 167.0 (s), 163.6 (s), 162.8 (d, <sup>1</sup> $J_{C-F} = 245.4$  Hz), 138.9 (s), 135.7 (d, <sup>5</sup> $J_{C-F} = 8.1$  Hz), 132.6 (s), 132.1 (d, <sup>4</sup> $J_{C-F} = 8.4$  Hz), 129.4 (s), 126.6 (d, <sup>6</sup> $J_{C-F} = 2.5$  Hz), 124.4 (s), 124.2 (s), 119.6 (s), 118.4 (d, <sup>3</sup> $J_{C-F} = 21.2$  Hz), 117.9 (d, <sup>2</sup> $J_{C-F} = 22.5$  Hz), 47.3 (s); HRMS (ESI) [M-H]<sup>-</sup> calcd for C<sub>18</sub>H<sub>12</sub>O<sub>2</sub>N<sub>2</sub>FS<sub>2</sub>: 371.0333, found: 371.0319.

*(Z)-2-(5-(3-chlorobenzylidene)-4-oxo-2-thioxothiazolidin-3-yl)-N-phenylacetamide (I<sub>8</sub>)*. A yellow solid, yield 51.0%, m.p. 255–256 °C; <sup>1</sup>H NMR (400 MHz, DMSO-d<sub>6</sub>) δ 10.44 (s, 1H, CO-NH-phenyl), 7.91 (s, 1H, CH-phenyl), 7.79 (s, 1H, phenyl-6-H), 7.64–7.59 (m, 3H, phenyl-3-H + phenyl-4-H + phenyl-5-H), 7.55 (d,  $J = 7.6$  Hz, 2H, NH-phenyl-2-H + NH-phenyl-6-H), 7.33 (t,  $J = 7.9$  Hz, 2H, NH-phenyl-3-H + NH-phenyl-5-H), 7.08 (t,  $J = 7.4$  Hz, 1H, NH-phenyl-4-H), 4.90 (s, 2H, CH<sub>2</sub>-CONH); <sup>13</sup>C NMR (101 MHz, DMSO-d<sub>6</sub>) δ 193.7 (s), 167.0 (s), 163.5 (s), 138.8 (s), 135.5 (s), 134.6 (s), 132.4 (s), 131.9 (s), 131.1 (s), 129.4 (s), 128.8 (s), 124.4 (s), 124.2 (s), 119.6 (s), 47.3 (s); HRMS (ESI) [M-H]<sup>-</sup> calcd for C<sub>18</sub>H<sub>12</sub>O<sub>2</sub>N<sub>2</sub>ClS<sub>2</sub>: 387.0038, found: 387.0023.

*(Z)-2-(5-(3-bromobenzylidene)-4-oxo-2-thioxothiazolidin-3-yl)-N-phenylacetamide (I<sub>9</sub>)*. A yellow solid, yield 59.0%, m.p. 264–265 °C; <sup>1</sup>H NMR (400 MHz, DMSO-d<sub>6</sub>) δ 10.43 (s, 1H, CO-NH-phenyl), 7.89 (s, 1H, CH-phenyl), 7.79 (d,  $J = 8.5$  Hz, 2H, phenyl-6-H + phenyl-5-H), 7.64 (d,  $J = 8.6$  Hz, 2H, phenyl-2-H + phenyl-4-H), 7.55 (d,  $J = 7.6$  Hz, 2H, NH-phenyl-2-H + NH-phenyl-6-H), 7.32 (t,  $J = 7.9$  Hz, 2H, NH-phenyl-3-H + NH-phenyl-5-H), 7.08 (t,  $J = 7.4$  Hz, 1H, NH-phenyl-4-H), 4.89 (s, 2H, CH<sub>2</sub>-CONH); <sup>13</sup>C NMR (101 MHz, DMSO-d<sub>6</sub>) δ 193.8 (s), 167.1 (s), 163.6 (s), 138.9 (s), 133.1 (s), 133.0 (s), 132.8 (s), 132.6 (s), 129.4 (s), 125.3 (s), 124.2 (s), 123.5 (s), 119.6 (s), 47.2 (s); HRMS (ESI) [M-H]<sup>-</sup> calcd for C<sub>18</sub>H<sub>12</sub>O<sub>2</sub>N<sub>2</sub>BrS<sub>2</sub>: 430.9534, found: 430.9518.

*(Z)-2-(5-(3-hydroxybenzylidene)-4-oxo-2-thioxothiazolidin-3-yl)-N-phenylacetamide (I<sub>10</sub>)*. A yellow solid, yield 39.0%, m.p. 252–253 °C; <sup>1</sup>H NMR (400 MHz, DMSO-d<sub>6</sub>) δ 10.44 (s, 1H, CO-NH-phenyl), 9.92 (s, 1H, OH-phenyl), 7.81 (s, 1H, CH-phenyl), 7.56 (d,  $J = 7.6$  Hz, 2H, NH-phenyl-2-H + NH-phenyl-6-H), 7.38 (t,  $J = 7.9$  Hz, 1H, phenyl-5-H), 7.33 (t,  $J = 8.0$  Hz, 2H, NH-phenyl-3-H + NH-phenyl-5-H), 7.14 (d,  $J = 7.7$  Hz, 1H, NH-phenyl-4-H), 7.11–7.04 (m, 2H, phenyl-5-H + phenyl-6-H), 6.95 (m, 1H, phenyl-2-H), 4.90 (s, 2H, CH<sub>2</sub>-CONH); <sup>13</sup>C NMR (101 MHz, DMSO-d<sub>6</sub>) δ 194.1 (s), 167.2 (s), 163.6 (s), 158.5 (s), 138.9 (s), 134.5 (s), 134.4 (s), 131.1 (s), 129.4 (s), 124.2 (s), 122.6 (s), 122.4 (s), 119.6 (s), 119.0 (s), 116.8 (s), 47.2 (s); HRMS (ESI) [M-H]<sup>-</sup> calcd for C<sub>18</sub>H<sub>13</sub>O<sub>3</sub>N<sub>2</sub>S<sub>2</sub>: 369.0375, found: 369.0362.

(*Z*)-2-(5-(3-methoxybenzylidene)-4-oxo-2-thioxothiazolidin-3-yl)-*N*-phenylacetamide (*I*<sub>11</sub>). A yellow solid, yield 44.0%, m.p. 226–227 °C; <sup>1</sup>H NMR (400 MHz, DMSO-*d*<sub>6</sub>) δ 10.44 (s, 1H, CO–NH-phenyl), 7.88 (s, 1H, CH-phenyl), 7.56 (d, *J* = 7.6 Hz, 2H, NH-phenyl-2-H + NH-phenyl-6-H), 7.50 (t, *J* = 8.2 Hz, 1H, phenyl-5-H), 7.33 (t, *J* = 8.0 Hz, 2H, NH-phenyl-3-H + NH-phenyl-5-H), 7.25 (dd, *J* = 4.0, 2.1 Hz, 2H, phenyl-2-H + phenyl-6-H), 7.13 (m, 1H, phenyl-4-H), 7.08 (t, *J* = 7.4 Hz, 1H, NH-phenyl-4-H), 4.90 (s, 2H, CH<sub>2</sub>–CONH), 3.84 (s, 3H, OCH<sub>3</sub>); <sup>13</sup>C NMR (101 MHz, DMSO-*d*<sub>6</sub>) δ 194.0 (s), 167.1 (s), 163.6 (s), 160.2 (s), 138.9 (s), 134.7 (s), 134.1 (s), 131.2 (s), 129.4 (s), 124.2 (s), 123.0 (s), 119.6 (s), 117.7 (s), 116.4 (s), 55.8 (s), 47.2 (s); HRMS (ESI) [M–H]<sup>–</sup> calcd for C<sub>19</sub>H<sub>15</sub>O<sub>3</sub>N<sub>2</sub>S<sub>2</sub>: 383.0534, found: 383.0519.

(*Z*)-2-(5-(4-nitrobenzylidene)-4-oxo-2-thioxothiazolidin-3-yl)-*N*-phenylacetamide (*I*<sub>12</sub>). A yellow solid, yield 53.0%, m.p. 240–241 °C; <sup>1</sup>H NMR (400 MHz, DMSO-*d*<sub>6</sub>) δ 10.45 (s, 1H, CO–NH-phenyl), 8.37 (d, *J* = 8.9 Hz, 2H, phenyl-3-H + phenyl-5-H), 8.01 (s, 1H, CH-phenyl), 7.95 (d, *J* = 8.8 Hz, 2H, phenyl-2-H + phenyl-6-H), 7.55 (d, *J* = 7.6 Hz, 2H, NH-phenyl-2-H + NH-phenyl-6-H), 7.33 (t, *J* = 8.0 Hz, 2H, NH-phenyl-3-H + NH-phenyl-5-H), 7.08 (t, *J* = 7.4 Hz, 1H, NH-phenyl-4-H), 4.91 (s, 2H, CH<sub>2</sub>–CONH); <sup>13</sup>C NMR (101 MHz, DMSO-*d*<sub>6</sub>) δ 193.6 (s), 166.9 (s), 163.5 (s), 148.3 (s), 139.4 (s), 138.9 (s), 132.1 (s), 131.2 (s), 129.4 (s), 126.9 (s), 124.9 (s), 124.2 (s), 119.6 (s), 47.3 (s); HRMS (ESI) [M–H]<sup>–</sup> calcd for C<sub>18</sub>H<sub>12</sub>O<sub>4</sub>N<sub>3</sub>S<sub>2</sub>: 398.0280, found: 398.0264.

(*Z*)-2-(4-oxo-2-thioxo-5-(4-(trifluoromethyl)benzylidene)thiazolidin-3-yl)-*N*-phenylacetamide (*I*<sub>13</sub>). A yellow solid, yield 63.0%, m.p. 246–247 °C; <sup>1</sup>H NMR (400 MHz, DMSO-*d*<sub>6</sub>) δ 10.45 (s, 1H, CO–NH-phenyl), 7.99 (s, 1H, CH-phenyl), 7.96–7.85 (m, 4H, phenyl-2-H + phenyl-3-H + phenyl-5-H + phenyl-6-H), 7.56 (d, *J* = 7.6 Hz, 2H, NH-phenyl-2-H + NH-phenyl-6-H), 7.33 (t, *J* = 7.9 Hz, 2H, NH-phenyl-3-H + NH-phenyl-5-H), 7.09 (t, *J* = 7.4 Hz, 1H, NH-phenyl-4-H), 4.92 (s, 2H, CH<sub>2</sub>–CONH); <sup>13</sup>C NMR (101 MHz, DMSO-*d*<sub>6</sub>) δ 193.7 (s), 167.0 (s), 163.5 (s), 138.9 (s), 137.2 (s), 132.0 (s), 131.6 (s), 130.6 (d, <sup>2</sup>*J*<sub>C–F</sub> = 32.0 Hz), 129.4 (s), 126.8 (s), 126.7 (d, <sup>3</sup>*J*<sub>C–F</sub> = 10.8 Hz), 126.7 (s), 124.9 (d, <sup>1</sup>*J*<sub>C–F</sub> = 145.7 Hz), 122.9 (s), 119.6 (s), 47.3 (s); HRMS (ESI) [M–H]<sup>–</sup> calcd for C<sub>19</sub>H<sub>12</sub>O<sub>2</sub>N<sub>2</sub>F<sub>3</sub>S<sub>2</sub>: 421.0302, found: 421.0287.

(*Z*)-2-(5-(4-fluorobenzylidene)-4-oxo-2-thioxothiazolidin-3-yl)-*N*-phenylacetamide (*I*<sub>14</sub>). A yellow solid, yield 52.0%, m.p. 273–274 °C; <sup>1</sup>H NMR (400 MHz, DMSO-*d*<sub>6</sub>) δ 10.43 (s, 1H, CO–NH-phenyl), 7.93 (s, 1H, CH-phenyl), 7.78 (dd, *J* = 8.8, 5.4 Hz, 2H, phenyl-3-H + phenyl-5-H), 7.55 (d, *J* = 7.6 Hz, 2H, NH-phenyl-2-H + NH-phenyl-6-H), 7.43 (t, *J* = 8.8 Hz, 2H, phenyl-2-H + phenyl-6-H), 7.32 (t, *J* = 7.9 Hz, 2H, NH-phenyl-3-H + NH-phenyl-5-H), 7.08 (t, *J* = 7.4 Hz, 1H, NH-phenyl-4-H), 4.90 (s, 2H, CH<sub>2</sub>–CONH); <sup>13</sup>C NMR (101 MHz, DMSO-*d*<sub>6</sub>) δ 193.9 (s), 167.1 (s), 163.8 (d, <sup>1</sup>*J*<sub>C–F</sub> = 252.0 Hz), 163.6 (s), 138.9 (s), 133.8 (d, <sup>3</sup>*J*<sub>C–F</sub> = 8.9 Hz), 133.0 (s), 130.1 (d, <sup>4</sup>*J*<sub>C–F</sub> = 3.2 Hz), 129.4 (s), 124.2 (s), 122.4 (s), 119.6 (s), 117.3 (d, <sup>2</sup>*J*<sub>C–F</sub> = 22.1 Hz), 47.2 (s); HRMS (ESI) [M–H]<sup>–</sup> calcd for C<sub>18</sub>H<sub>12</sub>O<sub>2</sub>N<sub>2</sub>F<sub>2</sub>S<sub>2</sub>: 371.0332, found: 371.0319.

(*Z*)-2-(5-(4-chlorobenzylidene)-4-oxo-2-thioxothiazolidin-3-yl)-*N*-phenylacetamide (*I*<sub>15</sub>). A yellow solid, yield 50.0%, m.p. 305–306 °C; <sup>1</sup>H NMR (400 MHz, DMSO-*d*<sub>6</sub>) δ 10.43 (s, 1H, CO–NH-phenyl), 7.91 (s, 1H, CH-phenyl), 7.72 (d, *J* = 8.6 Hz, 2H, phenyl-2-H + phenyl-6-H), 7.67–7.63 (m, 2H, phenyl-3-H + phenyl-5-H), 7.55 (d, *J* = 7.6 Hz, 2H, NH-phenyl-2-H + NH-phenyl-6-H), 7.32 (t, *J* = 8.0 Hz, 2H, NH-phenyl-3-H + NH-phenyl-5-H), 7.08 (t, *J* = 7.4 Hz, 1H, NH-phenyl-4-H), 4.89 (s, 2H, CH<sub>2</sub>–CONH); <sup>13</sup>C NMR (101 MHz, DMSO-*d*<sub>6</sub>) δ 193.8 (s), 167.1 (s), 163.6 (s), 138.9 (s), 136.3 (s), 132.8 (s), 132.7 (s), 132.3

(s), 130.1 (s), 129.4 (s), 124.2 (s), 123.4 (s), 119.6 (s), 47.2 (s); HRMS (ESI) [M–H]<sup>–</sup> calcd for C<sub>18</sub>H<sub>12</sub>O<sub>2</sub>N<sub>2</sub>ClS<sub>2</sub>: 387.0041, found: 387.0023.

(*Z*)-2-(5-(4-hydroxybenzylidene)-4-oxo-2-thioxothiazolidin-3-yl)-*N*-phenylacetamide (*I*<sub>16</sub>). A yellow solid, yield 21.0%, m.p. 270–271 °C; <sup>1</sup>H NMR (400 MHz, DMSO-*d*<sub>6</sub>) δ 10.43 (s, 1H, CO–NH-phenyl), 7.81 (s, 1H, CH-phenyl), 7.56 (dd, *J* = 8.1, 6.2 Hz, 4H, NH-phenyl-2-H + NH-phenyl-6-H + phenyl-2-H + phenyl-6-H), 7.32 (t, *J* = 8.0 Hz, 2H, NH-phenyl-3-H + NH-phenyl-5-H), 7.08 (t, *J* = 7.4 Hz, 1H, NH-phenyl-4-H), 6.96 (d, *J* = 8.7 Hz, 2H, phenyl-3-H + phenyl-5-H), 4.88 (s, 1H, CH<sub>2</sub>–CONH); <sup>13</sup>C NMR (101 MHz, DMSO-*d*<sub>6</sub>) δ 193.9 (s), 167.2 (s), 163.7 (s), 161.3 (s), 138.9 (s), 134.9 (s), 134.0 (s), 129.4 (s), 124.4 (s), 124.1 (s), 119.6 (s), 117.9 (s), 117.2 (s), 47.1 (s); HRMS (ESI) [M–H]<sup>–</sup> calcd for C<sub>18</sub>H<sub>13</sub>O<sub>3</sub>N<sub>2</sub>S<sub>2</sub>: 369.0375, found: 369.0362.

(*Z*)-2-(5-(4-isopropylbenzylidene)-4-oxo-2-thioxothiazolidin-3-yl)-*N*-phenylacetamide (*I*<sub>17</sub>). A yellow solid, yield 53.0%, m.p. 230–231 °C; <sup>1</sup>H NMR (400 MHz, DMSO-*d*<sub>6</sub>) δ 10.44 (s, 1H, CO–NH-phenyl), 7.88 (s, 1H, CH-phenyl), 7.62 (d, *J* = 8.3 Hz, 2H, phenyl-2-H + phenyl-6-H), 7.56 (d, *J* = 7.6 Hz, 2H, NH-phenyl-2-H + NH-phenyl-6-H), 7.46 (d, *J* = 8.3 Hz, 2H, phenyl-3-H + phenyl-5-H), 7.32 (t, *J* = 7.9 Hz, 2H, NH-phenyl-3-H + NH-phenyl-5-H), 7.08 (t, *J* = 7.4 Hz, 1H, NH-phenyl-4-H), 4.90 (s, 2H, CH<sub>2</sub>–CONH), 2.97 (dt, *J* = 13.7, 6.9 Hz, 1H, CH(CH<sub>3</sub>)<sub>2</sub>), 1.23 (d, *J* = 6.9 Hz, 6H, CH(CH<sub>3</sub>)<sub>2</sub>); <sup>13</sup>C NMR (101 MHz, DMSO-*d*<sub>6</sub>) δ 194.0 (s), 167.2 (s), 163.6 (s), 152.7 (s), 138.9 (s), 134.2 (s), 131.5 (s), 131.1 (s), 129.4 (s), 128.1 (s), 124.2 (s), 121.5 (s), 119.6 (s), 47.2 (s), 34.0 (s), 23.9 (s); HRMS (ESI) [M–H]<sup>–</sup> calcd for C<sub>21</sub>H<sub>19</sub>O<sub>2</sub>N<sub>2</sub>S<sub>2</sub>: 395.0896, found: 395.0882.

(*Z*)-2-(5-(4-methoxybenzylidene)-4-oxo-2-thioxothiazolidin-3-yl)-*N*-phenylacetamide (*I*<sub>18</sub>). A yellow solid, yield 31.0%, m.p. 257–258 °C; <sup>1</sup>H NMR (400 MHz, DMSO-*d*<sub>6</sub>) δ 10.43 (s, 1H, CO–NH-phenyl), 7.86 (s, 1H, CH-phenyl), 7.66 (d, *J* = 8.9 Hz, 2H, phenyl-2-H + phenyl-6-H), 7.56 (d, *J* = 7.7 Hz, 2H, NH-phenyl-2-H + NH-phenyl-6-H), 7.32 (t, *J* = 7.9 Hz, 2H, NH-phenyl-3-H + NH-phenyl-5-H), 7.15 (d, *J* = 8.9 Hz, 2H, phenyl-3-H + phenyl-5-H), 7.08 (t, *J* = 7.4 Hz, 1H, NH-phenyl-4-H), 4.89 (s, 2H, CH<sub>2</sub>–CONH), 3.86 (s, 3H, OCH<sub>3</sub>); <sup>13</sup>C NMR (101 MHz, DMSO-*d*<sub>6</sub>) δ 193.9 (s), 167.2 (s), 163.7 (s), 162.2 (s), 138.9 (s), 134.3 (s), 133.6 (s), 129.4 (s), 125.9 (s), 124.1 (s), 119.6 (s), 119.3 (s), 115.7 (s), 56.1 (s), 47.2 (s); HRMS (ESI) [M + Na]<sup>+</sup> calcd for C<sub>19</sub>H<sub>16</sub>O<sub>3</sub>N<sub>2</sub>S<sub>2</sub>: 407.0496, found: 407.0492.

(*Z*)-2-(5-(4-ethoxybenzylidene)-4-oxo-2-thioxothiazolidin-3-yl)-*N*-phenylacetamide (*I*<sub>19</sub>). A yellow solid, yield 58.0%, m.p. 270–271 °C; <sup>1</sup>H NMR (400 MHz, DMSO-*d*<sub>6</sub>) δ 10.42 (s, 1H, CO–NH-phenyl), 7.86 (s, 1H, CH-phenyl), 7.65 (d, *J* = 8.9 Hz, 2H, phenyl-2-H + phenyl-6-H), 7.55 (d, *J* = 7.6 Hz, 2H, NH-phenyl-2-H + NH-phenyl-6-H), 7.32 (t, *J* = 7.9 Hz, 2H, NH-phenyl-3-H + NH-phenyl-5-H), 7.13 (d, *J* = 8.8 Hz, 2H, phenyl-3-H + phenyl-5-H), 7.07 (t, *J* = 7.4 Hz, 1H, NH-phenyl-4-H), 4.88 (s, 2H, CH<sub>2</sub>–CONH), 4.14 (q, *J* = 7.0 Hz, 2H, OCH<sub>2</sub>CH<sub>3</sub>), 1.36 (t, *J* = 7.0 Hz, 3H, OCH<sub>2</sub>CH<sub>3</sub>); <sup>13</sup>C NMR (101 MHz, DMSO-*d*<sub>6</sub>) δ 193.9 (s), 167.2 (s), 163.7 (s), 161.5 (s), 138.92 (s), 134.4 (s), 133.6 (s), 129.4 (s), 125.8 (s), 124.1 (s), 119.6 (s), 119.2 (s), 116.1 (s), 64.2 (s), 47.2 (s), 15.0 (s); HRMS (ESI) [M–H]<sup>–</sup> calcd for C<sub>20</sub>H<sub>17</sub>O<sub>3</sub>N<sub>2</sub>S<sub>2</sub>: 397.0688, found: 397.0675.

(*Z*)-2-(5-(4-(dimethylamino)benzylidene)-4-oxo-2-thioxothiazolidin-3-yl)-*N*-phenylacetamide (*I*<sub>20</sub>). A orange solid, yield 48%, m.p. 227–228 °C; <sup>1</sup>H NMR (400 MHz, DMSO-*d*<sub>6</sub>) δ 10.41 (s, 1H, NH–CO), 7.73 (s, 1H, CH-phenyl), 7.55 (d, *J* = 8.0 Hz, 2H, NH-phenyl-2-H + NH-phenyl-6-H), 7.50 (d, *J* = 8.8 Hz, 2H, (CH<sub>3</sub>CH<sub>2</sub>)<sub>2</sub>N-phenyl-2-H + (CH<sub>3</sub>CH<sub>2</sub>)<sub>2</sub>N-phenyl-6-H), 7.32 (t, *J* = 7.9 Hz, 2H, NH-phenyl-3-

H + NH-phenyl-5-H), 7.07 (t,  $J = 7.4$  Hz, 1H, NH-phenyl-4-H), 6.84 (d,  $J = 8.6$  Hz, 2H,  $(\text{CH}_3\text{CH}_2)_2\text{N}$ -phenyl-3-H +  $(\text{CH}_3\text{CH}_2)_2\text{N}$ -phenyl-5-H), 4.87 (s, 2H, N- $\text{CH}_2$ -CO-NH), 3.46 (q,  $J = 6.9$  Hz, 4H,  $(\text{CH}_3\text{CH}_2)_2\text{N}$ -phenyl), 1.14 (t,  $J = 7.0$  Hz, 6H,  $(\text{CH}_3\text{CH}_2)_2\text{N}$ -phenyl);  $^{13}\text{C}$  NMR (101 MHz, DMSO- $d_6$ )  $\delta$  193.3 (s), 167.2 (s), 163.8 (s), 150.4 (s), 139.0 (s), 135.6 (s), 134.2 (s), 129.3 (s), 124.1 (s), 119.7 (s), 119.6 (s), 113.5 (s), 112.4 (s), 47.1 (s), 44.5 (s), 12.9 (s). HRMS (ESI)  $[\text{M} + \text{Na}]^+$  calcd for  $\text{C}_{22}\text{H}_{23}\text{N}_3\text{O}_2\text{S}_2$ : 448.1124, found: 448.1125.

**(Z)-2-(5-(2,4-dichlorobenzylidene)-4-oxo-2-thioxothiazolidin-3-yl)-N-phenylacetamide (I<sub>21</sub>)**. A yellow solid, yield 78.0%, m.p. 260–261 °C;  $^1\text{H}$  NMR (400 MHz, DMSO- $d_6$ )  $\delta$  10.44 (s, 1H, CO-NH-phenyl), 7.90 (d,  $J = 5.3$  Hz, 2H, CH-phenyl + phenyl-3-H), 7.64 (s, 2H, phenyl-5-H + phenyl-6-H), 7.54 (d,  $J = 7.6$  Hz, 2H, NH-phenyl-2-H + NH-phenyl-6-H), 7.32 (t,  $J = 7.9$  Hz, 2H, NH-phenyl-3-H + NH-phenyl-5-H), 7.08 (t,  $J = 7.4$  Hz, 1H, NH-phenyl-4-H), 4.89 (s, 2H,  $\text{CH}_2$ -CONH);  $^{13}\text{C}$  NMR (101 MHz, DMSO- $d_6$ )  $\delta$  193.6 (s), 166.8 (s), 163.5 (s), 138.9 (s), 136.7 (s), 136.2 (s), 131.2 (s), 130.6 (s), 130.3 (s), 129.4 (s), 129.1 (s), 127.5 (s), 126.8 (s), 124.2 (s), 119.6 (s), 47.3 (s); HRMS (ESI)  $[\text{M}-\text{H}]^-$  calcd for  $\text{C}_{18}\text{H}_{12}\text{O}_2\text{Cl}_2\text{N}_2\text{S}_2$ : 420.9654, found: 420.9634.

**(Z)-2-(5-(2-hydroxy-3-methoxybenzylidene)-4-oxo-2-thioxothiazolidin-3-yl)-N-phenylacetamide (I<sub>22</sub>)**. A yellow solid, yield 38%, m.p. 264–265 °C;  $^1\text{H}$  NMR (400 MHz, DMSO- $d_6$ )  $\delta$  10.43 (s, 1H, NH-CO), 10.03 (s, 1H, 2-OH-phenyl), 8.08 (s, 1H, phenyl-CH=C), 7.55 (d,  $J = 7.6$  Hz, 2H, NH-phenyl-2-H + NH-phenyl-6-H), 7.32 (t,  $J = 8.0$  Hz, 2H, phenyl-5-H + phenyl-6-H), 7.15 (dd,  $J = 7.8$ , 1.6 Hz, 1H, NH-phenyl-4-H), 7.08 (t,  $J = 7.4$  Hz, 1H, phenyl-4-H), 7.04–6.92 (m, 2H, NH-phenyl-3-H + NH-phenyl-5-H), 4.89 (s, 2H, N- $\text{CH}_2$ -CO-NH), 3.86 (s, 3H, 3-OCH<sub>3</sub>-phenyl);  $^{13}\text{C}$  NMR (101 MHz, DMSO- $d_6$ )  $\delta$  194.5 (s), 167.3 (s), 163.7 (s), 148.6 (s), 147.6 (s), 138.9 (s), 129.8 (s), 129.4 (s), 124.1 (s), 121.5 (s), 121.2 (s), 120.6 (s), 120.4 (s), 119.6 (s), 115.2 (s), 56.5 (s), 47.2 (s). HRMS (ESI)  $[\text{M} + \text{Na}]^+$  calcd for  $\text{C}_{19}\text{H}_{16}\text{N}_2\text{O}_4\text{S}_2$ : 423.0444, found: 423.0444.

**(Z)-2-(5-(cyclopropylmethylene)-4-oxo-2-thioxothiazolidin-3-yl)-N-phenylacetamide (I<sub>23</sub>)**. A yellow solid, yield 79.0%, m.p. 227–228 °C;  $^1\text{H}$  NMR (400 MHz, DMSO- $d_6$ )  $\delta$  10.39 (s, 1H, CO-NH-phenyl), 7.54 (d,  $J = 7.6$  Hz, 2H, NH-phenyl-2-H + NH-phenyl-6-H), 7.32 (t,  $J = 7.9$  Hz, 2H, NH-phenyl-3-H + NH-phenyl-5-H), 7.07 (t,  $J = 7.4$  Hz, 1H, NH-phenyl-4-H), 6.68 (d,  $J = 11.0$  Hz, 1H, CH-phenyl), 4.82 (s, 2H,  $\text{CH}_2$ -CONH), 1.65–1.54 (m, 1H, CH-CH<sub>2</sub>), 1.22–1.14 (m, 2H, CH-CH<sub>2</sub>), 1.05–0.99 (m, 2H, CH-CH<sub>2</sub>);  $^{13}\text{C}$  NMR (101 MHz, DMSO- $d_6$ )  $\delta$  194.4 (s), 165.2 (s), 163.7 (s), 146.6 (s), 138.9 (s), 129.3 (s), 124.1 (s), 122.4 (s), 119.6 (s), 47.0 (s), 16.4 (s), 11.1 (s); HRMS (ESI)  $[\text{M}-\text{H}]^-$  calcd for  $\text{C}_{15}\text{H}_{13}\text{O}_2\text{N}_2\text{S}_2$ : 314.0726, found: 314.0713.

**(Z)-2-(5-(furan-2-ylmethylene)-4-oxo-2-thioxothiazolidin-3-yl)-N-phenylacetamide (I<sub>24</sub>)**. A yellow solid, yield 82.0%, m.p. 255–256 °C;  $^1\text{H}$  NMR (400 MHz, DMSO- $d_6$ )  $\delta$  10.42 (s, 1H, CO-NH-phenyl), 8.18 (d,  $J = 1.6$  Hz, 1H, furanyl-3-H), 7.75 (s, 1H, CH-furanyl), 7.54 (d,  $J = 7.7$  Hz, 2H, NH-phenyl-2-H + NH-phenyl-6-H), 7.32 (t,  $J = 7.9$  Hz, 2H, NH-phenyl-3-H + NH-phenyl-5-H), 7.28 (d,  $J = 3.5$  Hz, 1H, furanyl-5-H), 7.08 (t,  $J = 7.4$  Hz, 1H, NH-phenyl-4-H), 6.82 (dd,  $J = 3.5$ , 1.8 Hz, 1H, furanyl-4-H), 4.87 (s, 2H,  $\text{CH}_2$ -CONH);  $^{13}\text{C}$  NMR (101 MHz, DMSO- $d_6$ )  $\delta$  194.9 (s), 166.8 (s), 163.7 (s), 150.0 (s), 149.4 (s), 138.9 (s), 129.4 (s), 124.1 (s), 121.4 (s), 119.9 (s), 119.6 (s), 119.3 (s), 114.6 (s), 47.1 (s); HRMS (ESI)  $[\text{M}-\text{H}]^-$  calcd for  $\text{C}_{16}\text{H}_{11}\text{O}_3\text{N}_2\text{S}_2$ : 343.0219, found: 343.0206.

**(Z)-2-(4-oxo-5-(thiophen-2-ylmethylene)-2-thioxothiazolidin-3-yl)-N-phenylacetamide (I<sub>25</sub>)**. A yellow solid, yield 76.0%, m.p. 277–278 °C;

$^1\text{H}$  NMR (400 MHz, DMSO- $d_6$ )  $\delta$  10.43 (s, 1H, CO-NH-phenyl), 8.20 (s, 1H, CH-thiophen-2-yl), 8.16 (d,  $J = 5.0$  Hz, 1H, thiophen-2-yl-3-H), 7.82 (d,  $J = 3.4$  Hz, 1H, thiophen-2-yl-5-H), 7.55 (d,  $J = 7.6$  Hz, 2H, NH-phenyl-2-H + NH-phenyl-6-H), 7.38–7.29 (m, 3H, NH-phenyl-3-H + NH-phenyl-5-H + thiophen-2-yl-4-H), 7.08 (t,  $J = 7.4$  Hz, 1H, NH-phenyl-4-H), 4.88 (s, 2H,  $\text{CH}_2$ -CONH);  $^{13}\text{C}$  NMR (101 MHz, DMSO- $d_6$ )  $\delta$  193.0 (s), 166.8 (s), 163.6 (s), 138.9 (s), 138.9 (s), 137.8 (s), 136.8 (s), 135.6 (s), 130.0 (s), 129.4 (s), 127.2 (s), 124.2 (s), 119.9 (s), 119.6 (s), 47.3 (s); HRMS (ESI)  $[\text{M}-\text{H}]^-$  calcd for  $\text{C}_{16}\text{H}_{12}\text{O}_2\text{N}_2\text{S}_2$ : 358.9366, found: 358.9377.

**(Z)-2-(5-((1H-pyrrol-2-yl)methylene)-4-oxo-2-thioxothiazolidin-3-yl)-N-phenylacetamide (I<sub>26</sub>)**. A yellow solid, yield 79.0%, m.p. 309–310 °C;  $^1\text{H}$  NMR (400 MHz, DMSO- $d_6$ )  $\delta$  10.42 (s, 1H, CO-NH-phenyl), 7.74 (s, 1H, CH-1H-pyrrol-2-yl), 7.55 (t,  $J = 7.4$  Hz, 2H, NH-phenyl-2-H + NH-phenyl-6-H), 7.43–7.38 (m, 1H, 1H-pyrrol-2-yl-5H), 7.37–7.29 (m, 3H, NH-phenyl-3-H + NH-phenyl-5-H + 1H-pyrrol-2-yl-NH), 7.07 (t,  $J = 7.4$  Hz, 1H, NH-phenyl-4-H), 6.67 (s, 1H, 1H-pyrrol-2-yl-3H), 6.45 (dd,  $J = 3.8$ , 2.0 Hz, 1H, 1H-pyrrol-2-yl-4H), 4.87 (s, 2H,  $\text{CH}_2$ -CONH);  $^{13}\text{C}$  NMR (101 MHz, DMSO- $d_6$ )  $\delta$  193.2 (s), 167.0 (s), 163.8 (s), 138.9 (s), 129.4 (s), 129.3 (s), 129.2 (s), 127.8 (s), 124.1 (s), 119.6 (s), 116.3 (s), 113.7 (s), 113.7 (s), 47.1 (s). HRMS (ESI)  $[\text{M} + \text{H}]^+$  calcd for  $\text{C}_{16}\text{H}_{13}\text{N}_3\text{O}_2\text{S}_2$ : 342.0376, found: 342.0380.

**(Z)-2-(5-(cyclohex-2-en-1-ylmethylene)-4-oxo-2-thioxothiazolidin-3-yl)-N-phenylacetamide (I<sub>27</sub>)**. A yellow solid, yield 52.0%, m.p. 171–172 °C;  $^1\text{H}$  NMR (400 MHz, DMSO- $d_6$ )  $\delta$  10.41 (s, 1H, CO-NH-phenyl), 7.54 (d,  $J = 7.6$  Hz, 2H, NH-phenyl-2-H + NH-phenyl-6-H), 7.32 (t,  $J = 7.9$  Hz, 2H, NH-phenyl-3-H + NH-phenyl-5-H), 7.07 (t,  $J = 7.4$  Hz, 1H, NH-phenyl-4-H), 7.01 (d,  $J = 9.6$  Hz, 1H, CH-phenyl), 4.88 (s, 2H,  $\text{CH}_2$ -CONH), 5.77–5.64 (m, 1H, cyclohex-2-en-1-yl-1-H), 2.54–2.42 (m, 2H, cyclohex-2-en-1-yl-4-H), 2.22–2.01 (m, 4H, cyclohex-2-en-1-yl-5-H + cyclohex-2-en-1-yl-6-H), 1.82–1.73 (m, 1H, cyclohex-2-en-1-yl-3-H), 1.67–1.53 (m, 1H, cyclohex-2-en-1-yl-2-H);  $^{13}\text{C}$  NMR (101 MHz, DMSO- $d_6$ )  $\delta$  194.5 (s), 165.8 (s), 163.6 (s), 143.6 (s), 138.9 (s), 129.3 (s), 127.4 (s), 125.2 (s), 124.1 (s), 119.6 (s), 47.1 (s), 37.4 (s), 29.3 (s), 26.8 (s), 23.9 (s); HRMS (ESI)  $[\text{M}-\text{H}]^-$  calcd for  $\text{C}_{18}\text{H}_{18}\text{O}_2\text{N}_2\text{S}_2$ : 357.0740, found: 357.0726.

**(Z)-2-(4-oxo-5-(pyridin-2-ylmethylene)-2-thioxothiazolidin-3-yl)-N-phenylacetamide (I<sub>28</sub>)**. A yellow solid, yield 83.0%, m.p. 315–316 °C;  $^1\text{H}$  NMR (400 MHz, DMSO- $d_6$ )  $\delta$  10.42 (s, 1H, CO-NH-phenyl), 8.83 (s, 1H, CH-phenyl), 7.95 (d,  $J = 22.0$  Hz, 3H, pyridin-2-yl-3-H + pyridin-2-yl-5-H + pyridin-2-yl-6-H), 7.61–7.43 (m, 3H, NH-phenyl-2-H + NH-phenyl-6-H + pyridin-2-yl-4-H), 7.32 (t,  $J = 7.4$  Hz, 2H, NH-phenyl-3-H + NH-phenyl-5-H), 7.07 (t,  $J = 7.0$  Hz, 1H, NH-phenyl-4-H), 4.89 (s, 2H,  $\text{CH}_2$ -CONH);  $^{13}\text{C}$  NMR (101 MHz, DMSO- $d_6$ )  $\delta$  200.4 (s), 167.2 (s), 163.8 (s), 151.5 (s), 150.1 (s), 138.9 (s), 138.3 (s), 129.6 (s), 129.4 (s), 128.9 (s), 127.0 (s), 124.8 (s), 124.1 (s), 119.6 (s), 46.8 (s); HRMS (ESI)  $[\text{M} + \text{H}]^+$  calcd for  $\text{C}_{17}\text{H}_{13}\text{O}_2\text{N}_3\text{S}_2$ : 356.0519, found: 356.0522.

**(Z)-2-(4-oxo-5-(pyridin-4-ylmethylene)-2-thioxothiazolidin-3-yl)-N-phenylacetamide (I<sub>29</sub>)**. A yellow solid, yield 66.0%, m.p. 285–286 °C;  $^1\text{H}$  NMR (400 MHz, DMSO- $d_6$ )  $\delta$  10.44 (s, 1H, CO-NH-phenyl), 8.76 (dd,  $J = 4.5$ , 1.6 Hz, 2H, pyridin-4-yl-2-H + pyridin-4-yl-6-H), 7.87 (s, 1H, CH-phenyl), 7.61 (dd,  $J = 4.7$ , 1.5 Hz, 2H, pyridin-4-yl-3-H + pyridin-4-yl-5-H), 7.55 (d,  $J = 7.6$  Hz, 2H, NH-phenyl-2-H + NH-phenyl-6-H), 7.32 (t,  $J = 7.9$  Hz, 2H, NH-phenyl-3-H + NH-phenyl-5-H), 7.08 (t,  $J = 7.4$  Hz, 1H, NH-phenyl-4-H), 4.90 (s, 2H,  $\text{CH}_2$ -CONH);  $^{13}\text{C}$  NMR (101 MHz, DMSO- $d_6$ )  $\delta$  193.6 (s), 166.9 (s), 163.5 (s), 151.3 (s), 140.2 (s), 138.9 (s), 130.9 (s), 129.4 (s), 127.7 (s), 124.2 (s), 119.7 (s), 47.3

(s); HRMS (ESI)  $[M-H]^-$  calcd for  $C_{17}H_{13}O_2N_3S_2$ : 354.0371, found: 354.0372.

*(Z)-2-(5-benzylidene-4-oxo-2-thioxothiazolidin-3-yl)-N-(3-methoxyphenyl)acetamide (I<sub>30</sub>)*. A yellow solid, yield 63.0%, m.p. 251–252 °C;  $^1H$  NMR (400 MHz, DMSO- $d_6$ )  $\delta$  10.45 (s, 1H, CO-NH-3-OCH<sub>3</sub>-phenyl), 7.91 (s, 1H, CH-phenyl), 7.70 (dd,  $J=8.0, 1.3$  Hz, 2H, phenyl-2-H + phenyl-6-H), 7.63–7.52 (m, 3H, phenyl-3-H + phenyl-5-H + 3-OCH<sub>3</sub>-phenyl-2-H), 7.29–7.18 (m, 2H, 3-OCH<sub>3</sub>-phenyl-6-H + 3-OCH<sub>3</sub>-phenyl-4-H), 7.07 (dd,  $J=8.1, 1.0$  Hz, 1H, phenyl-4-H), 6.67 (dd,  $J=8.2, 2.0$  Hz, 1H, 3-OCH<sub>3</sub>-phenyl-4-H), 4.89 (s, 2H, CH<sub>2</sub>-CONH), 3.72 (s, 3H, 3-OCH<sub>3</sub>-phenyl);  $^{13}C$  NMR (101 MHz, DMSO- $d_6$ )  $\delta$  194.1 (s), 167.1 (s), 163.7 (s), 160.0 (s), 140.1 (s), 134.2 (s), 133.3 (s), 131.7 (s), 131.2 (s), 130.2 (s), 130.1 (s), 122.6 (s), 111.8 (s), 109.8 (s), 105.2 (s), 55.5 (s), 47.2 (s); HRMS (ESI)  $[M+H]^+$  calcd for  $C_{19}H_{16}N_2O_3S_2$ : 385.0675, found: 385.0667.

*(Z)-2-(5-(4-fluorobenzylidene)-4-oxo-2-thioxothiazolidin-3-yl)-N-(3-methoxyphenyl)acetamide (I<sub>31</sub>)*. A yellow solid, yield 45.2%, m.p. 260–261 °C;  $^1H$  NMR (400 MHz, DMSO- $d_6$ )  $\delta$  10.45 (s, 1H, CO-NH-3-OCH<sub>3</sub>-phenyl), 7.93 (s, 1H, CH-4-F-phenyl), 7.78 (dd,  $J=8.8, 5.4$  Hz, 2H, 4-F-phenyl-2-H + 4-F-phenyl-6-H), 7.44 (t,  $J=8.8$  Hz, 2H, 4-F-phenyl-3-H + 4-F-phenyl-5-H), 7.27–7.20 (m, 2H, 3-OCH<sub>3</sub>-phenyl-2-H + 3-OCH<sub>3</sub>-phenyl-6-H), 7.07 (dd,  $J=7.9, 1.1$  Hz, 1H, 3-OCH<sub>3</sub>-phenyl-5-H), 6.67 (dd,  $J=8.1, 2.2$  Hz, 1H, 3-OCH<sub>3</sub>-phenyl-4-H), 4.89 (s, 2H, CH<sub>2</sub>-CONH), 3.72 (s, 3H, 3-OCH<sub>3</sub>-phenyl);  $^{13}C$  NMR (101 MHz, DMSO- $d_6$ )  $\delta$  193.9 (s), 167.1 (s), 163.8 (d,  $J=252.1$  Hz), 163.6 (s), 160.0 (s), 140.1 (s), 133.8 (d,  $J=9.0$  Hz), 133.1 (s), 130.2 (s), 130.1 (s), 130.1 (d,  $J=3.1$  Hz), 117.3 (d,  $J=22.1$  Hz), 111.8 (s), 109.8 (s), 105.2 (s), 55.5 (s), 47.2 (s); HRMS (ESI)  $[M+Na]^+$  calcd for  $C_{19}H_{15}FN_2O_3S_2$ : 425.0400, found: 425.0400.

*(Z)-2-(5-(cyclopropylmethylene)-4-oxo-2-thioxothiazolidin-3-yl)-N-(3-methoxyphenyl)acetamide (I<sub>32</sub>)*. A yellow solid, yield 71.2%, m.p. 195–196 °C;  $^1H$  NMR (400 MHz, DMSO- $d_6$ )  $\delta$  10.44 (s, 1H, CO-NH-3-OCH<sub>3</sub>-phenyl), 7.27 (dt,  $J=16.3, 5.1$  Hz, 2H, 3-OCH<sub>3</sub>-phenyl-2-H + 3-OCH<sub>3</sub>-phenyl-6-H), 7.10 (dd,  $J=8.1, 0.9$  Hz, 1H, 3-OCH<sub>3</sub>-phenyl-5-H), 6.74–6.64 (m, 2H, 3-OCH<sub>3</sub>-phenyl-4-H + CH-cyclopropyl), 4.85 (s, 2H, CH<sub>2</sub>-CONH), 3.75 (s, 3H, 3-OCH<sub>3</sub>-phenyl), 1.67–1.55 (m, 1H, cyclopropyl-1-H), 1.26–1.18 (m, 2H, cyclopropyl-3-H), 1.09–1.02 (m, 2H, cyclopropyl-2-H);  $^{13}C$  NMR (101 MHz, DMSO- $d_6$ )  $\delta$  194.3 (s), 165.2 (s), 163.7 (s), 160.0 (s), 146.6 (s), 140.1 (s), 130.2 (s), 122.4 (s), 111.8 (s), 109.7 (s), 105.2 (s), 55.4 (s), 46.9 (s), 16.4 (s), 11.1 (s); HRMS (ESI)  $[M+Na]^+$  calcd for  $C_{16}H_{16}N_2O_3S_2$ : 371.0495, found: 371.0497.

*(Z)-2-(5-(furan-2-ylmethylene)-4-oxo-2-thioxothiazolidin-3-yl)-N-(3-methoxyphenyl)acetamide (I<sub>33</sub>)*. A yellow solid, yield 71.2%, m.p. 221–222 °C;  $^1H$  NMR (400 MHz, DMSO- $d_6$ )  $\delta$  10.48 (s, 1H, CO-NH-furanyl), 8.21 (d,  $J=1.6$  Hz, 1H, furan-2-yl-5-H), 7.79 (s, 1H, CH-furan-2-yl), 7.33–7.22 (m, 3H, 3-OCH<sub>3</sub>-phenyl-2-H + furan-2-yl-3-H + furan-2-yl-4-H), 7.14–7.09 (m, 1H, 3-OCH<sub>3</sub>-phenyl-6-H), 6.86 (dd,  $J=3.5, 1.8$  Hz, 1H, 3-OCH<sub>3</sub>-phenyl-5-H), 6.70 (dd,  $J=8.2, 2.0$  Hz, 1H, 3-OCH<sub>3</sub>-phenyl-4-H), 4.91 (s, 2H, CH<sub>2</sub>-CONH), 3.76 (s, 3H, 3-OCH<sub>3</sub>-phenyl);  $^{13}C$  NMR (101 MHz, DMSO- $d_6$ )  $\delta$  194.9 (s), 166.8 (s), 163.7 (s), 160.0 (s), 150.0 (s), 149.4 (s), 140.1 (s), 130.2 (s), 121.4 (s), 119.9 (s), 119.3 (s), 114.6 (s), 111.8 (s), 109.7 (s), 105.2 (s), 55.4 (s), 47.1 (s); HRMS (ESI)  $[M+Na]^+$  calcd for  $C_{17}H_{14}N_2O_4S_2$ : 397.0287, found: 397.0289.

*(Z)-N-(3-methoxyphenyl)-2-(4-oxo-5-(thiophen-2-ylmethylene)-2-thioxothiazolidin-3-yl)acetamide (I<sub>34</sub>)*. A yellow solid, yield 48.2%, m.p.

243–244 °C;  $^1H$  NMR (400 MHz, DMSO- $d_6$ )  $\delta$  10.44 (s, 1H, CO-NH-thiophen-2-yl), 8.20 (s, 1H, CH-furan-2-yl), 8.17 (d,  $J=5.0$  Hz, 1H, thiophen-2-yl-5-H), 7.82 (d,  $J=3.6$  Hz, 1H, thiophen-2-yl-3-H), 7.36 (dd,  $J=5.0, 3.8$  Hz, 1H, thiophen-2-yl-4-H), 7.27–7.19 (m, 2H, 3-OCH<sub>3</sub>-phenyl-2-H + 3-OCH<sub>3</sub>-phenyl-6-H), 7.07 (dd,  $J=8.0, 1.1$  Hz, 1H, 3-OCH<sub>3</sub>-phenyl-5-H), 6.66 (dd,  $J=7.9, 2.3$  Hz, 1H, 3-OCH<sub>3</sub>-phenyl-4-H), 4.87 (s, 2H, CH<sub>2</sub>-CONH), 3.72 (s, 3H, 3-OCH<sub>3</sub>-phenyl);  $^{13}C$  NMR (101 MHz, DMSO- $d_6$ )  $\delta$  192.9 (s), 166.8 (s), 163.7 (s), 160.0 (s), 140.1 (s), 137.8 (s), 136.8 (s), 135.6 (s), 130.2 (s), 129.9 (s), 127.3 (s), 119.8 (s), 111.8 (s), 109.8 (s), 105.2 (s), 55.5 (s), 47.3 (s); HRMS (ESI)  $[M+H]^+$  calcd for  $C_{17}H_{14}N_2O_3S_3$ : 413.0059, found: 413.0066.

## Acknowledgements

The authors thank Anne M. O'Rourke (PhD) for supervising the draft of this manuscript.

## Disclosure statement

No potential conflict of interest was reported by the author(s).

## Funding

The authors acknowledge the financial supports of National Natural Science Foundation of China [21867004, 22007022], Science and Technology Foundation of Guizhou Province [ZK[2021]034], Frontiers Science Center for Asymmetric Synthesis and Medicinal Molecules, Department of Education, Guizhou Province [Qianjiaohe KY number (2020)004].

## ORCID

Xiang Zhou  <http://orcid.org/0000-0002-3589-9074>

Zhenchao Wang  <http://orcid.org/0000-0003-1859-0128>

## References

- David AR, Zimmerman MR. Cancer: an old disease, a new disease or something in between? *Nat Rev Cancer* 2010;10: 728–33.
- Yahya EB, Alqadhi AM. Recent trends in cancer therapy: a review on the current state of gene delivery. *Life Sci* 2021; 269:119087.
- Shi JF, Cao MM, Wang YT, et al. Is it possible to halve the incidence of liver cancer in China by 2050? *Int J Cancer* 2021;148:1051–65.
- Haq A, Sofi NY. Vitamin D and breast cancer: Indian perspective. *Clin Nutr Exp* 2017;12:1–10.
- Crume KP, O'Sullivan D, Miller JH, et al. Delaying the onset of experimental autoimmune encephalomyelitis with the microtubule-stabilizing compounds, paclitaxel and Peloruside A. *J Leukoc Biol* 2009;86:949–58.
- Lo YC, Cormier O, Liu T, et al. Pocket similarity identifies selective estrogen receptor modulators as microtubule modulators at the taxane site. *Nature Commun* 2019;10:1–10.
- Ali R, Mirza Z, Ashraf GM, et al. New anticancer agents: recent developments in tumor therapy. *Anticancer Res* 2012; 32:2999–3005.

8. Bartlett JB, Dredge K, Dalgleish AG. The evolution of thalidomide and its IMiD derivatives as anticancer agents. *Nat Rev Cancer* 2004;4:314–22.
9. Nogales E. Structural insight into microtubule function. *Annu Rev Biophys Biomol Struct* 2001;30:397–420.
10. Ilan Y. Microtubules: From understanding their dynamics to using them as potential therapeutic targets. *J Cell Physiol* 2019;234:7923–37.
11. Pasquier E, Kavallaris M. Microtubules: a dynamic target in cancer therapy. *IUBMB Life* 2008;60:165–70.
12. Jordan MA, Wilson L. Microtubules as a target for anticancer drugs. *Nat Rev Cancer* 2004;4:253–65.
13. Mukhtar E, Adhami VM, Mukhtar H. Targeting microtubules by natural agents for cancer therapy. *Mol Cancer Ther* 2014;13:275–84.
14. Steinmetz MO, Prota AE. Microtubule-targeting agents: strategies to hijack the cytoskeleton. *Trends Cell Biol* 2018;28:776–92.
15. Tangutur DA, Kumar D, Krishna KV, et al. Microtubule targeting agents as cancer chemotherapeutics: an overview of molecular hybrids as stabilizing and destabilizing agents. *Curr Top Med Chem* 2017;17:2523–37.
16. Liu YM, Chen HL, Lee HY, et al. Tubulin inhibitors: a patent review. *Expert Opin Ther Pat* 2014;24:69–88.
17. Naaz F, Haider MR, Shafi S, et al. Anti-tubulin agents of natural origin: Targeting Taxol, vinca, and colchicine binding domains. *Eur J Med Chem* 2019;171:310–31.
18. Cao YN, Zheng LL, Wang D, et al. Recent advances in microtubule-stabilizing agents. *Eur J Med Chem* 2018;143:806–28.
19. Shwetha B, Sudhanva MS, Jagadeesha GS, et al. Furan-2-carboxamide derivative, a novel microtubule stabilizing agent induces mitotic arrest and potentiates apoptosis in cancer cells. *Bioorg Chem* 2021;108:104586.
20. Zhang Q, Liu XJ, Li XE, et al. Antitumor activity of (2E,5Z)-5-(2-hydroxybenzylidene)-2-((4-phenoxyphenyl)imino) thiazolidin-4-one, a novel microtubule-depolymerizing agent, in U87MG human glioblastoma cells and corresponding mouse xenograft model. *J Pharmacol Sci* 2013;122:223–31.
21. Mu Y, Liu Y, Li LW, et al. The novel tubulin polymerization inhibitor MHPT exhibits selective anti-tumor activity against rhabdomyosarcoma in vitro and in vivo. *PLoS One* 2015;10:e0121806.
22. Marinho J, Pedro M, Pinto DC, et al. 4'-methoxy-2-styrylchromone a novel microtubule-stabilizing antimetabolic agent. *Biochem Pharmacol* 2008;75:826–35.
23. Leslie BJ, Holaday CR, Nguyen T, et al. Phenylcinnamides as novel antimetabolic agents. *J Med Chem* 2010;53:3964–72.
24. Baytas SN, Incel N, Yılmaz A, et al. Synthesis, biological evaluation and molecular docking studies of trans-indole-3-acrylamide derivatives, a new class of tubulin polymerization inhibitors. *Bioorg Med Chem* 2014;22:3096–104.
25. Reddy MR, Akula B, Cosenza SC, et al. (Z)-1-Aryl-3-arylamino-2-propen-1-ones, Highly Active Stimulators of Tubulin Polymerization: Synthesis, structure-activity relationship (SAR), tubulin polymerization, and cell growth inhibition studies. *J Med Chem* 2012;55:5174–87.
26. Haggarty SJ, Mayer TU, Miyamoto DT, et al. Dissecting cellular processes using small molecules: identification of colchicine-like, Taxol-like and other small molecules that perturb mitosis. *Chem Biol* 2000;7:275–86.
27. Woods JA, Hadfield JA, Pettit GR, et al. The interaction with tubulin of a series of stilbenes based on combretastatin A-4. *Br J Cancer* 1995;71:705–11.
28. Chen H, Li YM, Sheng CQ, et al. Design and synthesis of cyclopropylamide analogues of combretastatin-A4 as novel microtubule-stabilizing agents. *J Med Chem* 2013;56:685–99.
29. Kim DY, Kim KH, Kim ND, et al. Design and biological evaluation of novel tubulin inhibitors as antimetabolic agents using a pharmacophore binding model with tubulin. *J Med Chem* 2006;49:5664–70.
30. Greene TF, Wang S, Greene LM, et al. Synthesis and biochemical evaluation of 3-Phenoxy-1,4-diazepin-2-ones as Tubulin-Targeting Antitumor Agents. *J Med Chem* 2016;59:90–113.
31. Chopra A, Anderson A, Giardina C. Novel piperazine-based compounds inhibit microtubule dynamics and sensitize colon cancer cells to tumor necrosis factor-induced apoptosis. *J Biol Chem* 2014;289:2978–91.
32. Řehulka J, Vychodilová K, Krejčí P, et al. Fluorinated derivatives of 2-phenyl-3-hydroxy-4(1H)-quinolinone as tubulin polymerization inhibitors. *Eur J Med Chem* 2020;192:112176.
33. Scholey JM, Brust-Mascher I, Mogilner A. Cell division. *Nature* 2003;422:746–52.
34. Bastiaens P, Caudron M, Niethammer P, et al. Gradients in the self-organization of the mitotic spindle. *Trends Cell Biol* 2006;16:125–34.
35. Rodriguez OC, Schaefer AW, Mandato CA, et al. Conserved microtubule-actin interactions in cell movement and morphogenesis. *Nat Cell Biol* 2003;5:599–609.
36. Pellegrini F, Budman DR. Review: tubulin function, action of antitubulin drugs, and new drug development. *Cancer Invest* 2005;23:264–73.
37. Lu YX, Wang Y, Zhu WL. Nonbonding interactions of organic halogens in biological systems: implications for drug discovery and biomolecular design. *Phys Chem Chem Phys* 2010;12:4543–51.
38. Johnson ER, Keinan S, Mori-Sánchez P, et al. Revealing Noncovalent Interactions. *J Am Chem Soc* 2010;132:6498–506.
39. Mahadevi AS, Sastry GN. Cooperativity in Noncovalent Interactions. *Chem Rev* 2016;116:2775–825.
40. Zhou X, Feng YM, Qi PY, et al. Synthesis and docking study of N-(Cinnamoyl)-N'-(substituted)acryloyl hydrazide derivatives containing pyridinium moieties as a novel class of filamentous temperature-sensitive protein Z inhibitors against the intractable xanthomonas oryzae pv. oryzae INFECTIONS IN RICE. *J Agric Food Chem* 2020;68:8132–42.
41. Zhou X, Ye YQ, Liu SS, et al. Design, synthesis and anti-TMV activity of novel  $\alpha$ -aminophosphonate derivatives containing a chalcone moiety that induce resistance against plant disease and target the TMV coat protein. *Pestic Biochem Physiol* 2021;172:104749.
42. Friedl P, Wolf K. Tumour-cell invasion and migration: diversity and escape mechanisms. *Nat Rev Cancer* 2003;3:362–74.
43. Berges R, Tchoghandjian A, Honoré S, et al. The novel tubulin-binding checkpoint activator BAL101553 inhibits EB1-dependent migration and invasion and promotes differentiation of glioblastoma stem-like cells. *Mol Cancer Ther* 2016;15:2740–9.
44. Etienne-Manneville S. Microtubules in cell migration. *Annu Rev Cell Dev Biol* 2013;29:471–99.
45. Watanabe T, Noritake J, Kaibuchi K. Regulation of microtubules in cell migration. *Trends Cell Biol* 2005;15:76–83.
46. Le Y, Gan YY, Fu YH, et al. Design, synthesis and in vitro biological evaluation of quinazolinone derivatives as EGFR

- inhibitors for antitumor treatment. *J Enzyme Inhib Med Chem* 2020;35:555–64.
47. Gao F, Liang Y, Zhou PF, et al. Design, synthesis, antitumor activities and biological studies of novel diaryl substituted fused heterocycles as dual ligands targeting tubulin and katanin. *Eur J Med Chem* 2019;178:177–94.
  48. Bai HH, Jin H, Yang F, et al. Apigenin induced MCF-7 cell apoptosis-associated reactive oxygen species. *Scanning* 2014;36:622–31.
  49. Zhang YW, Zhao HB, Di YC, et al. Antiproliferative activity of Pinoresinol in vitro: Inducing apoptosis and inhibiting HepG2 invasion. *J Funct Foods* 2018;45:206–14.
  50. Zhang C, Qu Y, Ma X, et al. NQO1-selective activated prodrugs of combretastatin A-4: synthesis and biological evaluation. *Bioorg Chem* 2020;103:104200.
  51. Risinger AL, Li J, Bennett MJ, et al. Taccalonolide Binding to Tubulin Imparts Microtubule Stability and Potent *In Vivo* Activity. *Cancer Res* 2013;73:6780–92.
  52. Feng YJ, Ren YL, Zhao LM, et al. Design, synthesis and biological evaluation of novel  $\alpha$ -acyloxycarboxamide-based derivatives as c-met inhibitors. *Chinese J Chem* 2021;39:2241–2250.
  53. Wu YY, Shao WB, Zhu JJ, et al. Novel 1,3,4-oxadiazole-2-carbohydrazides as prospective agricultural antifungal agents potentially targeting succinate dehydrogenase. *J Agric Food Chem* 2019;67:13892–903.
  54. Wu ZB, Park HY, Xie DW, et al. Synthesis, biological Evaluation, and 3D-QSAR studies of *N*-(Substituted pyridine-4-yl)-1-(substituted phenyl)-5-trifluoromethyl-1H-pyrazole-4-carboxamide derivatives as potential succinate dehydrogenase inhibitors. *J Agric Food Chem* 2021;69:1214–23.
  55. Hu X, Li L, Zhang QS, et al. Design, synthesis and biological evaluation of a novel tubulin inhibitor SKLB0565 targeting the colchicine binding site. *Bioorg Chem* 2020;97:103695.
  56. Zhang XN, Breslav M, Grimm J, et al. A new procedure for preparation of carboxylic acid hydrazides. *J Org Chem* 2002;67:9471–4.